Quaternary Science Reviews 373 (2026) 109746

Contents lists available at ScienceDirect

Quaternary Science Reviews

journal homepage: www.elsevier.com/locate/quascirev

Paleoenvironments of the late Middle Pleistocene Hualongdong, east-central China and their implications for the hominin evolution in eastern Asia

Jiao Ma [a,b,*], Hervé Bocherens [c,d], Haowen Tong [a,e], Shuwen Pei [a,b], Xiujie Wu [a,b,**], Wu Liu [a,b]

[a] Key Laboratory of Vertebrate Evolution and Human Origins of Chinese Academy of Sciences, Institute of Vertebrate Paleontology and Paleoanthropology, Chinese Academy of Sciences, Beijing, 100044, China
[b] Key Scientific Research Base on Paleolithic Human Evolution and Paleogenetics (IVPP), SACH, Beijing, 100044, China
[c] Senckenberg Centre for Human Evolution and Palaeoenvironment (HEP), Universität Tübingen, Tübingen, 72074, Germany
[d] Fachbereich Geowissenschaften, Forschungsbereich Paläobiologie, Universität Tübingen, Tübingen, 72074, Germany
[e] University of Chinese Academy of Sciences, Beijing, China

ARTICLE INFO

Handling Editor: Donatella Magri

Keywords:
Stable isotopes
Tooth enamel
Late Middle Pleistocene
Hualongdong
Paleoenvironment
Eastern Asia

ABSTRACT

The late Middle Pleistocene (300–129 ka) was pivotal for understanding how paleoenvironmental and climatic changes shaped hominin adaptations. Hualongdong (331–275 ka) yields key human fossils, stone tools, and abundant mammalian remains, enabling detailed paleoecological analysis. Carbon isotopic data from mammalian tooth enamel indicate a C_3 vegetation-dominated forest environment at Hualongdong. The isotopic composition of a large bovid indicates, however, the co-existence of year-round C_4 grasses. Bulk and serial isotopic results reveal a mosaic of dense forests and woodlands shaped by the East Asian Summer Monsoon (EASM). Closed forests would have provided stable resources, while seasonally dynamic woodlands with localized C_4 vegetation would have supported favorable conditions for habitation and movement. Comparative analyses of Middle Pleistocene enamel stable isotopes across eastern Asia (including East and Southeast Asia) highlight distinct paleoenvironments in northern, east-central, southwestern China, as well as in Southeast Asia. Hualongdong in east-central China stands out as a mosaic of dense forests and open woodlands, distinct from the open woodlands of north China and the dense forests of southwestern China. The Hualongdong hominins exhibit a mosaic of derived and archaic traits, representing a significant morphological pattern in the late Middle Pleistocene of eastern Asia. Their successful occupation of this ecotonal landscape as revealed by our isotopic data, underscores the behavioral flexibility that characterized hominin evolution in this region.

1. Introduction

A central challenge of human evolutionary studies is understanding the role of climatic change in shaping Middle Pleistocene hominin environments and selective pressures (Maslin et al., 2014). In Africa, the emergence of *Homo sapiens* during the late Middle Pleistocene (300–129 ka) and its subsequent spread toward Eurasia have attracted multidisciplinary attention (White et al., 2003; Hershkovitz et al., 2018; Harvati et al., 2019). In China, an increasing number of late Middle Pleistocene fossil records highlights the morphological and genetic diversities of hominin fossils (Chen et al., 2019; Liu et al., 2022; Bae and Wu, 2024; Fu et al., 2025). As a crucial period along the pathway of human evolution, the Middle Pleistocene climatic transition may be the underlying factor behind human lineage diversification and hominin behavioral development (Pearson, 2013; Ao et al., 2020; Yang et al., 2021; Qin and Sun, 2023). While global studies have advanced Pleistocene paleoclimatic and paleoenvironmental reconstructions (Louys and Roberts, 2020; Foerster et al., 2022; Gosling et al., 2022), direct ecological evidence

* Corresponding author. Key Laboratory of Vertebrate Evolution and Human Origins of Chinese Academy of Sciences, Institute of Vertebrate Paleontology and Paleoanthropology, Chinese Academy of Sciences, Beijing, 100044, China.
** Corresponding author. Key Laboratory of Vertebrate Evolution and Human Origins of Chinese Academy of Sciences, Institute of Vertebrate Paleontology and Paleoanthropology, Chinese Academy of Sciences, Beijing, 100044, China.
E-mail addresses: majiao@ivpp.ac.cn (J. Ma), wuxiujie@ivpp.ac.cn (X. Wu).

https://doi.org/10.1016/j.quascirev.2025.109746
Received 15 September 2025; Received in revised form 16 November 2025; Accepted 3 December 2025
Available online 7 December 2025
0277-3791/© 2025 The Authors. Published by Elsevier Ltd. This is an open access article under the CC BY license (http://creativecommons.org/licenses/by/4.0/).

linking hominin behavior to regional environmental variability remains scarce in eastern Asia.

Stable isotope analysis provides quantitative geochemical data from mammalian tooth enamel and has long been a powerful tool for reconstructing paleoecology and paleoenvironments (Kohn and Cerling, 2002). A major benefit of analyzing mammalian tooth enamel is the possibility of utilizing carbon and oxygen isotope records from the same fossil collections in which hominin specimens or stone tools have been found, yielding insights into climate and ecology at spatial scales directly relevant to hominin environments. This is an advantage over offsite sedimentary sequences, which have limited applicability for understanding ecology and environmental conditions at a local scale. As one of the most commonly-used approaches, stable isotope analysis has been widely applied in archaeological and paleontological sites in Asia (Suraprasit et al., 2018; Ma et al., 2019a; Louys and Roberts, 2020; Bacon et al., 2023). These methods have opened a new window on the Quaternary climatic and environmental changes in Asia but simultaneously raised new questions regarding our incomplete knowledge of the mammalian assemblage evolution and chronological framework. It is regrettable that most isotopic analyses were carried out on a limited number of often patchy Quaternary sites, a challenge that also affects the discontinuous records of Chinese faunas (Zeitoun et al., 2023). So far, this approach has never been directly applied to paleoecological study of absolute-dated, human-bearing faunas with high-resolution age constraints in late Middle Pleistocene China, which has limited our understanding of the relationship between human evolution and paleoenvironmental changes in eastern Asia.

The Hualongdong site (331–275 ka) offers a unique opportunity to address this gap. Its well-dated deposits preserve the earliest Middle Pleistocene hominins in East Asia with significant modern human features documented in the regional fossil record, alongside diverse mammalian fossils and stone tools (Wu et al., 2019; Liu and Wu, 2025). The Hualongdong faunal assemblage, comprising 93 species, is broadly comparable to the classic *Ailuropoda-Stegodon* fauna of southern China, yet exhibits a transitional character marked by a mixture of northern and southern taxa (Tong et al., 2018, 2025). In this study, we conducted stable carbon and oxygen isotope analysis on mammalian fossils from the Hualongdong fauna to investigate the habitats exploited by its hominins. Additionally, we synthesized published isotopic data to provide a deeper understanding of the relationship between paleoecological settings and hominin evolution in eastern Asia during the Middle Pleistocene.

2. The principles of stable carbon and oxygen isotopes

Terrestrial vegetation is classified into three photosynthetic pathways: C_3 (most trees, shrubs, herbs, and cool-season grasses), C_4 (warm-season grasses), and CAM (e.g. succulents), which yield distinct $\delta^{13}C$ values due to differences in carbon fixation biochemistry (Troughton and Card, 1975; O'Leary, 1981; Farquhar et al., 1989). Modern C_3 plants exhibit an average $\delta^{13}C$ value of −25 ‰, whereas C_4 plants average −13 ‰ (Bender, 1968; Smith and Epsten, 1971). Variability in plant $\delta^{13}C$ arises from environmental factors such as water use efficiency, canopy density, and climatic conditions (van der Merwe and Medina, 1991; Kohn, 2010). These isotopic signatures propagate through food webs, resulting in a systematic enrichment during metabolic processing. In mammalian tooth enamel, carbon isotope discrimination typically ranges from 12 ‰ to 15 ‰, relative to dietary sources, and is modulated by trophic level, digestive physiology, and body size (Cerling and Harris, 1999; Passey et al., 2005; Tejada-Lara et al., 2018; Cerling et al., 2021).

The oxygen isotope composition ($\delta^{18}O$) of bioapatite reflects the $\delta^{18}O$ of body water, which is primarily governed by ingested water and secondarily by dietary structural oxygen (Bryant and Froelich, 1995; Kohn et al., 1996). Regional precipitation $\delta^{18}O$ exhibits spatiotemporal heterogeneity, which is largely governed by temperature dependence at mid-high latitudes and precipitation amount effects in monsoonal systems (Pederzani and Britton, 2019). In the East Asia monsoon region, summer precipitation shows $\delta^{18}O$ minima due to intense convective rainfall, creating pronounced seasonal isotopic cycles in precipitation $\delta^{18}O$ values (Dutton et al., 2005; Biasatti et al., 2010). Herbivore enamel $\delta^{18}O$ records these environmental signals but is further modulated by dietary water resources; browsers consuming transpiration-enriched foliage typically have higher $\delta^{18}O$ values than grazers (Koch et al., 1989; Quade et al., 1995). It should be noted that $\delta^{18}O$ values can vary systematically between early- and late-forming teeth due to breast-feeding and weaning practices (Wright and Schwarcz, 1998, 1999).

These environmental signals become encoded in incrementally formed biological archives such as tooth enamel. Enamel bioapatite largely preserves its original isotopic composition post-mineralization (Suga, 1979; Hillson, 2005), enabling two analytical approaches: bulk sampling, which provides a time-averaged isotopic signal, and serial micro-sampling along the growth axis, which resolves seasonal-scale variation (Kohn et al., 1998; Balasse, 2002; Blumenthal et al., 2014). However, non-linear, layer-specific trajectories of enamel mineralization complicate precise temporal resolution, necessitating careful interpretation of isotopic sequences (Sharp and Cerling, 1998; Green et al., 2018). Despite these complexities, serial $\delta^{18}O$ data primarily track seasonal cycles in precipitation, temperature, and humidity, while serial $\delta^{13}C$ data can reveal seasonal dietary shifts.

3. Materials and method

3.1. Site background, stratigraphy, and faunal assemblage

The Hualongdong site (30°06′34.1″ N, 116°56′54.2″ E, 40 m above sea level, asl) is a karst cave located in Dongzhi County, Anhui Province, China (Wu et al., 2019) (Fig. 1). This cave, developed in Upper Cambrian limestone, contains a 5.5-m-thick sequence of poorly stratified archaeological deposits cemented by calcareous formations, which has yielded an extensive assemblage of hominin fossils, stone tools, and mammalian remains (Pei et al., 2022).

U-series dating of speleothems and fossil teeth constrains the primary occupation phase to the late Middle Pleistocene, between 331 and 275 ka (Wu et al., 2019). Recent flowstone analyses indicate a more complex depositional history, with an early phase of sedimentation earlier than 600 ka and a later phase from ca. 331 to 275 ka (Cai et al., 2025). This complexity is underscored by the presence of a molar from *Ailuropoda wulingshanensis*, a species typically found in late Early Pleistocene contexts, suggesting some stratigraphic mixing (Tong et al., 2025). Nevertheless, the overall biostratigraphic character and the evolutionary stage of the carnivore guild strongly support a late Middle Pleistocene age for the main assemblage (Tong et al., 2018, 2025; Jiangzuo et al., 2025).

The Hualongdong faunal assemblage comprises 93 mammalian species from 27 families and is broadly comparable to the classic *Ailuropoda-Stegodon* fauna of southern China. The dominant taxa include *Bos* (*Bibos*) sp. and several cervids (*Muntiacus* sp., *Cervus grayi*, and *Rusa unicolor*) (Tong et al., 2018, 2025). However, the fauna exhibits a distinct ecological transitional character, incorporating typically northern species such as *Ursus arctos*, *Equus* sp., *Sus lydekkeri*, and *Sinomegaceros* sp., which here represent their southernmost known occurrence in eastern China. These northern elements coexist with classic southern, forest-adapted taxa like *Ailuropoda baconi, Macaca sp., Neofelis nebulosa, Megatapirus augustus*, and *Arctonyx collaris rostratus*. This species composition indicates a mosaic habitat of forests and more open environments.

Evidence for hominin activity at Hualongdong is multifaceted. More than a decade of excavations has uncovered over 50 human fossils (including one well-preserved skull), stone tools, and other traces of human activity (Liu and Wu, 2025; Pei et al., 2025). A thorough taphonomic study reveals that cervid and bovid astragali bear anthropogenic cut and chopping marks, alongside carnivore tooth marks and rodent gnawing traces, suggesting the involvement of multiple agents in the

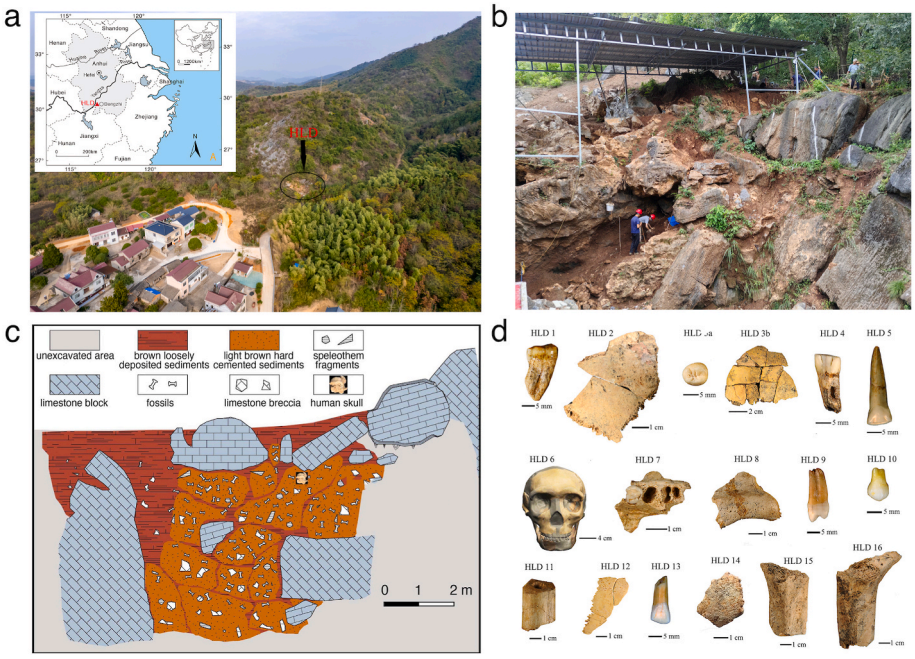

Fig. 1. Site overview of Hualongdong (HLD), Anhui Province, China. (a) Regional map showing the geographic position of the site (Wu et al., 2019). (b) Aerial view of the Hualongdong cave entrance and surrounding topography. (c) Longitudinal stratigraphic section of the deposits, showing the *in situ* location of the human skull (Wu et al., 2019). (d) Photographs of representative hominin fossils excavated from the site (Liu and Wu, 2025).

accumulation and modification of the bone assemblage (S. Liu et al., 2025). Analysis of large bovid dental fossils suggests that Hualongdong hominins employed flexible hunting strategies, potentially including a combination of ambush and endurance hunting, with a possible focus on juvenile individuals (B. Liu et al., 2025).

In summary, despite indications of limited stratigraphic mixing, the primary Hualongdong assemblage represents a well-dated and rich record of late Middle Pleistocene hominin occupation and its associated fauna. The evidence points to a mosaic ecosystem and offers crucial insights into hominin subsistence behavior in eastern Asia during this key period.

3.2. Sampling strategy

In this study, forty tooth enamel specimens from 11 mammalian taxa were analyzed, including *Bos* (*Bibos*) sp. (n = 6), *Bubalus* sp. (n = 1), *Cervus grayi* (n = 6), *Muntiacus* sp. (n = 4), *Sus* sp. (n = 5), Rhinocerotidae indet. (n = 6), *Stegodon orientalis* (n = 2), *Ailuropoda melanoleuca baconi* (n = 3), *Macaca* sp. (n = 4), *Crocuta* sp. (n = 2), and *Pachycrocuta* sp. (n = 1). Among the 40 teeth, we conducted serial sampling on four M2/3 M of *Bos* (*Bibos*) sp. and four M2/3 M of *Cervus grayi* as these tooth positions minimize breastfeeding and weaning effects, generating 66 samples. Combined with bulk-sampled specimens, a total of 98 enamel samples were analyzed for their carbon and oxygen isotopic composition. Here, a specimen refers to an individual tooth, while a sample denotes a discrete portion of enamel powder prepared for isotopic analysis (including both bulk and serial samplings). Additionally, 12 other tooth specimens from Ursidae (data for which were recently published; Ma et al., 2025), were included to obtain a complete paleoecology: *A. m. baconi* (n = 5), *Ursus thibetanus* (n = 4), and *Ursus arctos* (n = 3).

3.3. Bioapatite preparation and stable isotopic analysis

All samples were pretreated at the Institute of Vertebrate Paleontology and Paleoanthropology, Chinese Academy of Sciences (IVPP, CAS). First, the teeth were cleaned by removing a very thin (~0.1 mm) outer enamel layer using a diamond-tipped dental drill. For bulk sampling, enamel powder was collected across the entire tooth height to obtain an average isotopic value. For serial sampling, each sample was obtained by drilling a 1–2 mm-wide groove nearly perpendicular to the tooth growth axis, penetrating through the full enamel thickness at ca. 1–2 mm intervals. Approximately 12–15 mg of enamel powder was collected per sample in 1.5 mL centrifuge tubes.

All enamel powder samples were then pretreated with 2.5 % NaOCl followed by 1 M acetic acid (Bocherens et al., 1996; Ambrose et al., 1997). Aliquots of 3–5 mg were then analyzed at the Laboratory for Stable Isotope Geochemistry, Institute of Geology and Geophysics, Chinese Academy of Sciences using a MAT 253 IRMS coupled with a Gasbench unit. International standards (IAEA CO-8, NBS-19) were included in each run to establish a calibration curve. The in-house standard GBW04405 (limestone) and sample replicates were also analyzed to monitor measurement uncertainty. Carbon and oxygen isotope results were reported as $\delta^{13}C$ and $\delta^{18}O$ values relative to VPDB. Analytical precision, based on IAEA CO-8, NBS-19, and GBW04405, was better than ±0.15 ‰ ($\delta^{13}C$) and 0.20 ‰ ($\delta^{18}O$).

3.4. Data processing and statistical analysis

The carbon isotope enrichment factor ($\varepsilon^*_{diet\text{-}bioapatite}$) in mammals typically ranges between 12 ‰ and 15 ‰, due to interspecific differences in foraging strategies, digestive physiology, and body mass (Cerling and Harris, 1999; Passey et al., 2005; Tejada-Lara et al., 2018; Cerling et al., 2021). In this study, we employed species-specific enrichment factors based on digestive fermentation types (foregut *vs.* hindgut fermenters) using body mass (BM, kg)-calibrated formulae proposed by Tejada-Lara et al. (2018), aligning with regional standardization protocols for Quaternary eastern Asia (Bacon et al., 2021, 2023; Suraprasit et al., 2024). The calculation formulae are as follows:

$$\text{General}: \varepsilon^*_{diet-}bioapatite = e^{2.4+0.034(\ln BM)}$$

$$\text{Foregut fermenter}: \varepsilon^*_{diet-bioapatite} = e^{2.34+0.05(\ln BM)}$$

Hindgut fermenter : $\varepsilon^*_{\text{diet-bioapatite}} = e^{2.42+0.032(\ln BM)}$

Given the physiological incompatibility of direct $\varepsilon^*_{\text{diet-bioapatite}}$ calculations for carnivores, we adopted the carnivore-herbivore enamel $\delta^{13}C$ spacing value of 1.3 ‰ (Clementz et al., 2009). This offset was applied to carnivore $\delta^{13}C$ values to reconstruct prey bioapatite $\delta^{13}C$, which was subsequently converted to environmental $\delta^{13}C$ using the general formulae (Tejada-Lara et al., 2018). For ursids (except giant pandas), neither standard herbivore formulae nor carnivore proxy methods were applicable due to their omnivore physiology and lack of strict trophic specialization. We therefore used a $\varepsilon^*_{\text{diet-bioapatite}}$ value of 13.3 ‰ derived from suid studies (Passey et al., 2005; Bacon et al., 2021), selected as the most physiologically analogous omnivore reference. For the giant panda (*Ailuropoda* sp.), a specialized $\varepsilon^*_{\text{diet-bioapatite}}$ value of 10 ‰ was adopted based on controlled modern feeding experiments (Han et al., 2016).

After correction, we interpreted mammalian habitats using $\delta^{13}C_{\text{diet}}$ thresholds commonly applied in recent Southeast Asian studies (Kohn, 2010; Tejada et al., 2020; Bacon et al., 2021; Suraprasit et al., 2024): $\delta^{13}C_{\text{diet}} < -27.2$ ‰ for closed-canopy forests; −27.2 ‰ to −21.3 ‰ for intermediate rainforests/woodlands; −21.3 ‰ to −15.3 ‰ for intermediate area between open forests and savanna; and > −15.3 ‰ for open savanna.

Statistical analyses were performed using R version 4.5.1 (R Core Team, 2025). Pairwise comparisons were conducted using Mann-Whitney U tests with Bonferroni correction for multiple comparisons. Data visualizations were generated using Microsoft Excel, R with ggplot2 (Wickham, 2011) and ggpubr (Kassambara, 2020) packages, and QGIS 3.34 (QGIS Development Team, 2024).

4. Results and interpretations

4.1. Bulk carbon and oxygen isotope results

Stable carbon and oxygen isotope analysis was performed on 52 tooth specimens from Hualongdong. The measured $\delta^{13}C$ values range from −18.8 ‰ to −7.0 ‰, and $\delta^{18}O$ values span from −10.1 ‰ to −5.5 ‰ (Fig. 2, Table S1). After applying species-specific fractionation factors, the calculated $\delta^{13}C_{\text{diet}}$ values (−30.8 ‰ to −20.9 ‰) indicate that the entire herbivore community relied on C_3-based diets, consistent with foraging in closed-canopy forests to intermediate rainforests and woodlands (Kohn, 2010; Tejada et al., 2020; Bacon et al., 2021). The total range of enamel $\delta^{18}O$ values (ca. 5 ‰) signifies diverse water sources and physiological adaptations among the taxa.

Among the herbivores, *Bos* (*Bibos*) sp. specimens exhibit the highest mean $\delta^{13}C_{\text{diet}}$ values (−25.8 ± 3.4 ‰, n = 6) and substantial isotopic variability (−30.8 ‰ to −21.5 ‰), indicating considerable ecological flexibility across forest-woodland gradients. Two out of the six individuals have $\delta^{13}C_{\text{diet}}$ values higher than −23.0 ‰ (Kohn, 2010), suggesting minor C_4 grass consumption. Their $\delta^{18}O$ values range from −8.6 ‰ to −6.3 ‰ (mean = −7.3 ± 0.9 ‰), indicating varied water resources. Pleistocene Asian large bovids consistently display such ecological plasticity (Suraprasit et al., 2018; Bacon et al., 2021, 2023; Shaikh et al., 2025). One *Bubalus* sp. specimen ($\delta^{13}C_{\text{diet}}$ = −30.1 ‰, $\delta^{18}O$ = −8.3 ‰) falls within the lower ends of the *Bos* (*Bibos*) sp. ranges, with more negative isotopic values consistent with the ecology of buffalo in water-abundant, closed-canopy habitats.

Cervus grayi specimens display the second-highest mean $\delta^{13}C_{\text{diet}}$ values (−26.5 ± 1.9 ‰, n = 6), with a wide range of $\delta^{18}O$ values (−7.0 ± 1.3 ‰), suggesting a mixed-feeding ecology and diverse water resources from both foliage and meteoric water. In contrast, *Muntiacus* sp. shows lower $\delta^{13}C_{\text{diet}}$ values (−27.1 ± 1.7 ‰, n = 4), supporting a forest-specialized foraging ecology consistent with fossil and modern analogues (Hemami et al., 2004; MacCullough et al., 2009; Bacon et al., 2021). Their $\delta^{18}O$ values (−7.6 ± 1.0 ‰) are slightly lower than those of *Bos* (*Bibos*) sp. and *C. grayi* specimens, possibly because small *Muntiacus* sp. foraged under denser canopy, whereas the larger taxa could access vegetation from more open habitats or from higher canopy strata.

Rhinocerotidae indet. specimens (*Dicerorhinus sumatrensis/Stephanorhinus* sp.; Tong et al., 2018, 2025) exhibit a mean $\delta^{13}C_{\text{diet}}$ values of −28.2 ± 0.6 ‰ (n = 6), whereas the two *Stegodon orientalis* specimens have $\delta^{13}C_{\text{diet}}$ values of −30.0 ‰ and −29.7 ‰; both taxa show similar $\delta^{18}O$ values (approximately −7.2 ‰), implying forest-dwelling habitats and similar water resources. This aligns with browsing preferences of the extant Sumatran rhinoceros (Louys, 2008; Ahrestani et al., 2016) and fossil *Stegodon* and *Stephanorhinus* (Ma et al., 2019a; Stefaniak et al., 2021).

Sus sp. displays intermediate $\delta^{13}C_{\text{diet}}$ values (−26.9 ± 0.8 ‰, n = 5) but notably low $\delta^{18}O$ values (−8.8 ± 1.0 ‰). A similar pattern observed at the Middle Pleistocene Yugongdong in Guangxi, China (Sun et al., 2019) may reflect substantial meteoric water consumption and/or preferential use of ^{18}O-depleted resources, such as underground plant parts or animal proteins (Sternberg, 1989; Yakir, 1992). *Macaca* sp. shows $\delta^{13}C_{\text{diet}}$ and $\delta^{18}O$ values of −26.7 ± 0.6 ‰ and −7.7 ± 0.3 ‰ (n = 4), respectively, with the narrowest isotopic ranges among mammalian taxa with more than three specimens, indicating a specialized ecological niche, likely at forest edges.

Hyaenids exhibit clustered $\delta^{13}C_{\text{diet}}$ values, with two *Crocuta* sp. specimens at −29.4 ‰ and −28.4 ‰ and one *Pachycrocuta* sp. specimen at −29.5 ‰, consistent with predation on forest-dwelling herbivores such as cervids. Their low $\delta^{18}O$ values (<−8.0 ‰) likely derive from ^{18}O-

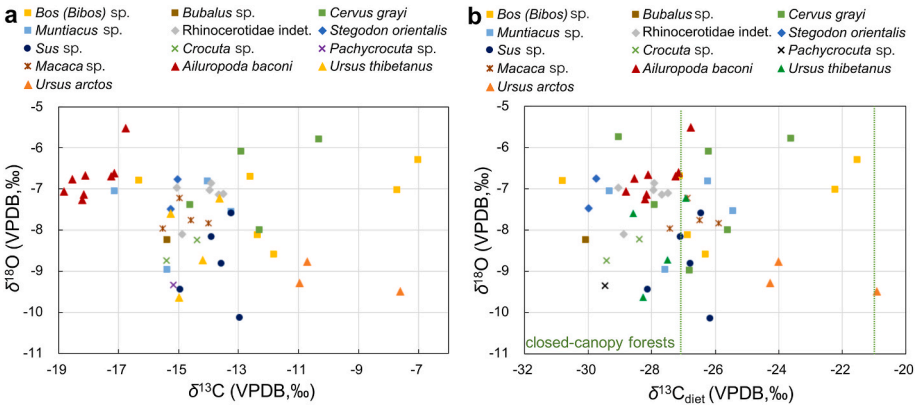

Fig. 2. Carbon and oxygen isotopic composition of mammalian fossils from Hualongdong. (a) $\delta^{13}C$ and $\delta^{18}O$ values measured from tooth enamel. (b) Reconstructed $\delta^{13}C_{\text{diet}}$ and $\delta^{18}O$ values with ecological divisions (Kohn, 2010; Tejada et al., 2020; Bacon et al., 2021) (closed-canopy forests: $\delta^{13}C_{\text{diet}<}-27.2$ ‰; intermediate rainforests/woodlands: $\delta^{13}C_{\text{diet}} > -27.2$ ‰ and < -21.3 ‰). Data for 12 ursids specimens were sourced from Ma et al. (2025). For *Bos* (*Bibos*) sp. and *Cervus grayi*, bulk samples and the mean values of each serial sample are all included.

depleted animal tissues (Sponheimer and Lee-Thorp, 1999, 2001).

Giant panda (*A. m. baconi*) specimens yield the lowest $\delta^{13}C$ values (−17.9 ± 0.7 ‰, n = 8) but the highest $\delta^{18}O$ values (−6.7 ± 0.6 ‰). Applying a taxon-specific fractionation factor (10 ‰; Han et al., 2016; Tejada-Lara et al., 2018), the resulting $\delta^{13}C_{diet}$ values (−27.9 ± 0.7 ‰) are similar to those of *Ursus thibetanus* specimens (−27.8 ± 0.7 ‰, n = 4), suggesting both species occupied closed forests. However, the wide range of $\delta^{18}O$ values in *U. thibetanus* (−8.3 ± 1.1 ‰) suggests greater dietary diversity. The high $\delta^{18}O$ values in *A. m. baconi* possibly indicate dependence on plant-derived water (Ma et al., 2025). The Hualongdong panda data align with those from Early Pleistocene southern Chinese sites (e.g., Yanliang Cave, Longgu Cave, and *Gigantopithecus* Cave), indicating potential ecological conservation of panda during the Pleistocene (Stacklyn et al., 2017; Jiang et al., 2021). *Ursus arctos* specimens exhibit the highest $\delta^{13}C_{diet}$ values (−23.1 ± 1.9 ‰, n = 3; Ma et al., 2025), indicating woodland habitat use. Their low $\delta^{18}O$ values resemble those of Hyaenids, reflecting a carnivorous feeding ecology (Sponheimer and Lee-Thorp, 1999, 2001).

In summary, the $\delta^{13}C_{diet}$ values of these taxa reflect a wide spectrum of dietary ecology: *Bos* (*Bibos*) sp. and *U. arctos* occupied the most open environments, whereas *Muntiacus* sp., Rhinocerotidae indet., *A. m. baconi, and Stegodon orientalis* inhabited closed canopy areas. A clear spatial spectrum is also evident in $\delta^{18}O$ values: taxa with the highest $\delta^{18}O$ values (e.g., *A. m. baconi*, *Bos* (*Bibos*) sp.) likely foraged in open habitats or accessed canopy-top vegetation, both of which are associated with ^{18}O-enriched water sources due to high evaporation. In contrast, species with the lowest $\delta^{18}O$ values (e.g., *Sus* sp., Hyaenids, *U. arctos*) consistently obtained water either from ^{18}O-depleted sources, such as underground plant tissues, or from prey body fluids.

4.2. Serial isotopic analysis

The serial isotopic profiles of the eight specimens examined in this study are summarized in Table 1 and displayed in Fig. 3. The four *Bos* (*Bibos*) sp. specimens exhibit intra-tooth $\delta^{13}C$ variations of 1.6–2.4 ‰ and $\delta^{18}O$ variations of 0.2–2.5 ‰. An inverse correlation between $\delta^{13}C$ and $\delta^{18}O$ values is observed in three out of four specimens (H1-01: $r = -0.5$, $p = 0.05$; H1-89: $r = -0.7$, $p = 0.01$; H1-03: $r = -0.5$, $p > 0.05$). Based on an enamel growth rate ca. 40 mm yr^{-1} derived from bison (Fricke and O'Neil, 1996), these variations enable sub-annual reconstructions of the species' ecology and of paleoclimatic and paleoenvironmental seasonality.

The four *C. grayi* specimens showed smaller variations ($\delta^{13}C$: 0.7–1.8 ‰; $\delta^{18}O$: 0.7–1.9 ‰) than the *Bos* (*Bibos*) sp. individuals (Table 1), which may be partially attributable to their shorter available tooth crown heights. In arid environments, smaller ungulates often exhibit larger isotopic variations and are considered better indicators of local seasonality than large obligate drinkers (Roberts et al., 2018; Ma et al., 2024). However, at Hualongdong, *C. grayi* exhibits weaker isotopic seasonality than sympatric *Bos* (*Bibos*) sp. This pattern is in contrast with observations from arid regions and suggests inhabitation of dense forests with attenuated seasonal fluctuations. The inverse $\delta^{13}C$-$\delta^{18}O$ relationship occurred only in H1-07 ($r = -0.9$, $p = 0.03$). The isotopic variation among the four *C. grayi* individuals indicates the ecological flexibility of this taxon.

As outlined in Section 2, isotopic variations in hypsodont teeth can preserve sub-annual climatic signals. Consistent with this principle, modern precipitation near Hualongdong (Nanjing/Wuhan) exhibits an annual $\delta^{18}O$ range of ca. 8 ‰, with the lowest values occurring in July during peak rainfall (Fig. 4). Although physiological processes and sampling constraints attenuate the recorded amplitude in *Bos* (*Bibos*) sp. enamel to ≤2.5 ‰, two specimens (H1-01 and H1-89) display sinusoidal $\delta^{18}O$ profiles that closely mirror this precipitation seasonality (Fig. 3). This suggests that these individuals were possibly non-migratory and accurately recorded local hydrologic seasonality. In contrast, the dampened $\delta^{18}O$ variations in the other two individuals may reflect ingestion of buffered water sources, such as lakes, rivers, or groundwater, or possible migratory behavior, which could integrate water sources from multiple locations (Pederzani and Britton, 2019). Although the intra-tooth $\delta^{18}O$ variations of the *C. grayi* specimens are smaller than those of *Bos* (*Bibos*) sp., their profiles still exhibit systematic directional trends, such as monotonic increase or decrease, that correspond to partial segments of the seasonal precipitation cycle, indicating preservation of sub-annual climatic seasonality.

Furthermore, the observed inverse correlations between $\delta^{13}C$ and $\delta^{18}O$ values align with the expected pattern under the East Asia Summer Monsoon (EASM). Enhanced summer precipitation simultaneously induced $\delta^{18}O$ depletion while promoted C_4 plant growth, leading to seasonal dietary shifts that generate such negative correlations (Higgins and MacFadden, 2004; Yang Wang et al., 2008; Biasatti et al., 2010; Yang et al., 2012; Ciner et al., 2015). Therefore, these correlations observed in *Bos* (*Bibos*) sp. and *C. grayi* specimens confirm EASM influence and localized C_4 plant distribution in Hualongdong (Biasatti et al., 2010; Ma et al., 2024). The summer monsoon inferred from the serial samples was consistent with other paleoclimatic proxies (Yongjin Wang et al., 2008).

Notably, specimen H1-04 exhibits the smallest intra-tooth isotopic variations ($\delta^{13}C$: −7.5 ‰ to −5.9 ‰; $\delta^{18}O$: −6.4 ‰ to −6.2 ‰) and no inverse correlation. Its high mean $\delta^{18}O$ value implies reliance on distinctive water resources, potentially indicative of migratory behavior (Roberts et al., 2018; Ma et al., 2024). Crucially, its $\delta^{13}C$ profile indicates year-round availability of C_4 grasses at Hualongdong, whereas other specimens consumed predominantly C_3 plants annually. This further underscores the ecological flexibility of *Bos* (*Bibos*) sp. and reinforces the finding of a mosaic environment at this site.

In summary, stable isotope evidence from the Hualongdong mammalian fauna indicates a mosaic ecosystem of C_3-dominated closed forests and woodlands, with localized C_4 vegetation sustained by the EASM. This study provides a detailed paleoecological and climatic context for the Hualongdong hominins, who inhabited this diverse, monsoon-influenced landscape.

Table 1
Summary of the serial isotopic results.

Lab No	Taxon	Tooth position	Sample amounts	$\delta^{13}C$				$\delta^{18}O$				R
				Mean/‰	Min/‰	Max/‰	Range/‰	Mean/‰	Min/‰	Max/‰	Range/‰	
H1-01	*Bos* (*Bibos*) sp.	M3	15	−16.3	−17.2	−14.8	2.4	−6.8	−8.2	−5.7	2.5	**−0.5**
H1-03	*Bos* (*Bibos*) sp.	m3	11	−11.8	−12.7	−10.5	2.2	−8.6	−9.2	−7.8	1.4	**−0.5**
H1-04	*Bos* (*Bibos*) sp.	m3	8	−7	−7.5	−5.9	1.6	−6.3	−6.4	−6.2	0.2	0.3
H1-89	*Bos* (*Bibos*) sp.	m2	12	−12.6	−13.5	−11.4	2.1	−6.7	−7.4	−6.1	1.3	**−0.7**
H1-06	*Cervus grayi*	m3	4	−14.6	−15	−14	1	−7.4	−8.1	−6.2	1.9	0.7
H1-07	*Cervus grayi*	M2	5	−12.9	−13.9	−12.1	1.8	−6.1	−6.9	−5.3	1.6	**−0.9**
H1-87	*Cervus grayi*	m3	5	−10.3	−10.8	−9.7	1.1	−5.5	−5.8	−5.1	0.7	0.5
H1-88	*Cervus grayi*	m3	6	−12.3	−12.6	−11.9	0.7	−7.4	−8	−6.9	1.1	−0.1

Table 2
Pairwise comparisons of $\delta^{13}C_{diet}$ values among Middle Pleistocene eastern Asian sites.

	Quzai Cave[a]	Baxian Cave	Coc Muoi	Cobra Cave	Yugongdong	Hualongdong	Pha Bong	Tham Wiman Nakin	Khok Sung	Zhoukoudian
Baxian Cave[b,c]										
Coc Muoi[d]										
Cobra Cave[e]	**	***	***							
Yugongdong[c]				*						
Hualongdong[f,g]		**								
Pha Bong[h,i]	***	***	***	***	***	***				
Tham Wiman Nakin[h,i,j]	***	***	***	**	***	***				
Khok Sung[j,k]	***	***	***	***	***	***				
Zhoukoudian[l]	***	***	***		***	***	***		**	
Trinil[m,n]	***	***	***	***	***	***		**	**	***

Values represent adjusted *p*-values from Mann-Whitney *U* tests with Bonferroni correction. Significance levels: *p < 0.05, **p < 0.01, ***p < 0.001. Empty cells indicate non-significant differences (p ≥ 0.05). Complete pairwise *p*-values are provided in Supplementary Table S3.
References.
[a] Ma et al. (2019).
[b] Ma et al. (2017).
[c] Sun et al. (2019).
[d] Bacon et al. (2021).
[e] Bacon et al. (2023).
[f] This study.
[g] Ma et al. (2025).
[h] Bocherens et al. (2017).
[i] Suraprasit et al. (2020).
[j] Pushkina et al. (2010).
[k] Suraprasit et al. (2018).
[l] Gaboardi et al. (2005).
[m] Janssen et al. (2016).
[n] Puspaningrum et al. (2020).

5. Discussion

5.1. Paleoenvironmental heterogeneity across Middle Pleistocene (774–129 ka) eastern Asia

Growing mammalian isotopic datasets offer a powerful tool for quantitative paleoenvironmental reconstruction and comparison. Eleven Middle Pleistocene sites in eastern Asia provide suitable enamel $\delta^{13}C$ and $\delta^{18}O$ values for a detailed assessment (Table S2). The following discussion utilizes $\delta^{13}C_{diet}$ values corrected using taxon-specific fractionation factors (Section 3.4, Table S2). While analytical protocol differences across different laboratories may introduce minor biases (Passey et al., 2007; Snoeck and Pellegrini, 2015; Pellegrini and Snoeck, 2016), these are likely negligible in broader-scale comparisons of large datasets (Jiang et al., 2020).

Fig. 5 compiles mammalian stable isotopic data from eleven eastern Asian sites (see map in Fig. 6), including Hualongdong, Baxian Cave, Quzai Cave, Yugongdong, Khok Sung, Pha Bong, Tham Wiman Nakin, Cobra Cave, Coc Muoi, Zhoukoudian and Trinil. To ensure robust comparisons, we focus on sites with comprehensive large-mammal datasets; localities with limited taxa or samples (Wang et al., 2007; Li et al., 2017) were excluded.

The $\delta^{13}C_{diet}$ values of Zhoukoudian fauna (layers 3–13 in Locality 1, ca. 720–470 ka) differ significantly from most of these sites (Table 2, S3) (Gaboardi et al., 2005). Unlike the C_3-dominated ecosystems of South China, the $\delta^{13}C_{diet}$ values of the Zhoukoudian fauna (−23.0 ± 3.8 ‰, −27.8 ‰ to −15.4 ‰, n = 53) indicate intermediate woodlands with mixed C_3/C_4 vegetation. The wide $\delta^{18}O$ range (−13.5 ‰ to −0.7 ‰) at Zhoukoudian may reflect temporal disparities across sampled stratigraphic layers. In contrast to the semi-open landscapes of North China, the *H. erectus*-bearing Trinil site in Java (540–430 ka) exhibits the highest $\delta^{13}C_{diet}$ values (−14.7 ± 2.7 ‰, −26.0 ‰ to −10.6 ‰, n = 55), suggesting a savanna-like environment characterized by extensive C_4 grasslands interspersed with patches of intermediate forests/woodlands (Joordens et al., 2015; Janssen et al., 2016; Puspaningrum et al., 2020).

For the three Guangxi sites, no statistical differences were observed in $\delta^{13}C_{diet}$ and $\delta^{18}O$ values (Tables 2 and 3, S3, S4) (Ma et al., 2017, 2019a; Sun et al., 2019). Based on artiodactyls and *Rhinoceros* biostratigraphy, Yugongdong (Gongjishan) dates to the late Middle Pleistocene (no younger than early Late Pleistocene) (Dong et al., 2014; Yan et al., 2023). The faunal assemblages at Baxian and Quzai caves resemble those at Zhiren Cave (ca. 110 ka; Jin et al., 2009), leading to their initial classification as early Late Pleistocene in previous studies (Ma et al., 2017, 2019a; Sun et al., 2019; Yan et al., 2023). However, Ge et al. (2020) suggest Zhiren Cave may be older (190–130 ka). Recent multi-method dating constrained the Guangxi cave ages: we adopted these absolute dates while pending future refinements through integrated faunal, anthropological, and chronological studies (Yingqi Zhang et al., 2024). Yugongdong dates to ca. 252–200 ka, slightly earlier than both Quzai (214–187 ka) and Baxian (200–143 ka) caves (Yingqi Zhang et al., 2024). The similarly low $\delta^{13}C_{diet}$ values at Yugongdong (−28.2 ± 2.6 ‰, n = 29), Quzai (−28.8 ± 2.6 ‰, n = 40), and Baxian Caves (−29.1 ± 2.1 ‰, n = 57) indicate the presence of closed-canopy forests in southwestern China, with no significant temporal variations.

Hualongdong (331–275 ka) predates these Guangxi sites. The mean $\delta^{13}C_{diet}$ values of the Hualongdong fauna (−27.2 ± 2.1 ‰, −30.8 ‰ to −20.9 ‰, n = 52) are significantly higher than those at Baxian Cave, and slightly higher than those from Yugongdong and Quzai Cave (Table 2, S3). Additionally, the minimum $\delta^{13}C_{diet}$ value at Hualongdong (−30.8 ‰) is higher than the values recorded at three Guangxi sites (all < −33.0 ‰). These findings suggest that the forests in Guangxi were characterized by denser canopy cover compared to Hualongdong (Ma et al., 2017, 2019a; Sun et al., 2019). This indicates that while south China generally supported closed-canopy forests with minor C_4 components, Hualongdong (east-central China) exhibited slightly more open landscapes than Guangxi (southwest China). These differences are not attributable to altitude, as all four sites are at low elevations (<200 m asl).

Coc Muoi mammals (148–117 ka, northern Vietnam) show $\delta^{13}C_{diet}$ (−28.3 ± 2.3 ‰, n = 84) and $\delta^{18}O$ (−6.2 ± 1.2 ‰) values (Bacon et al.,

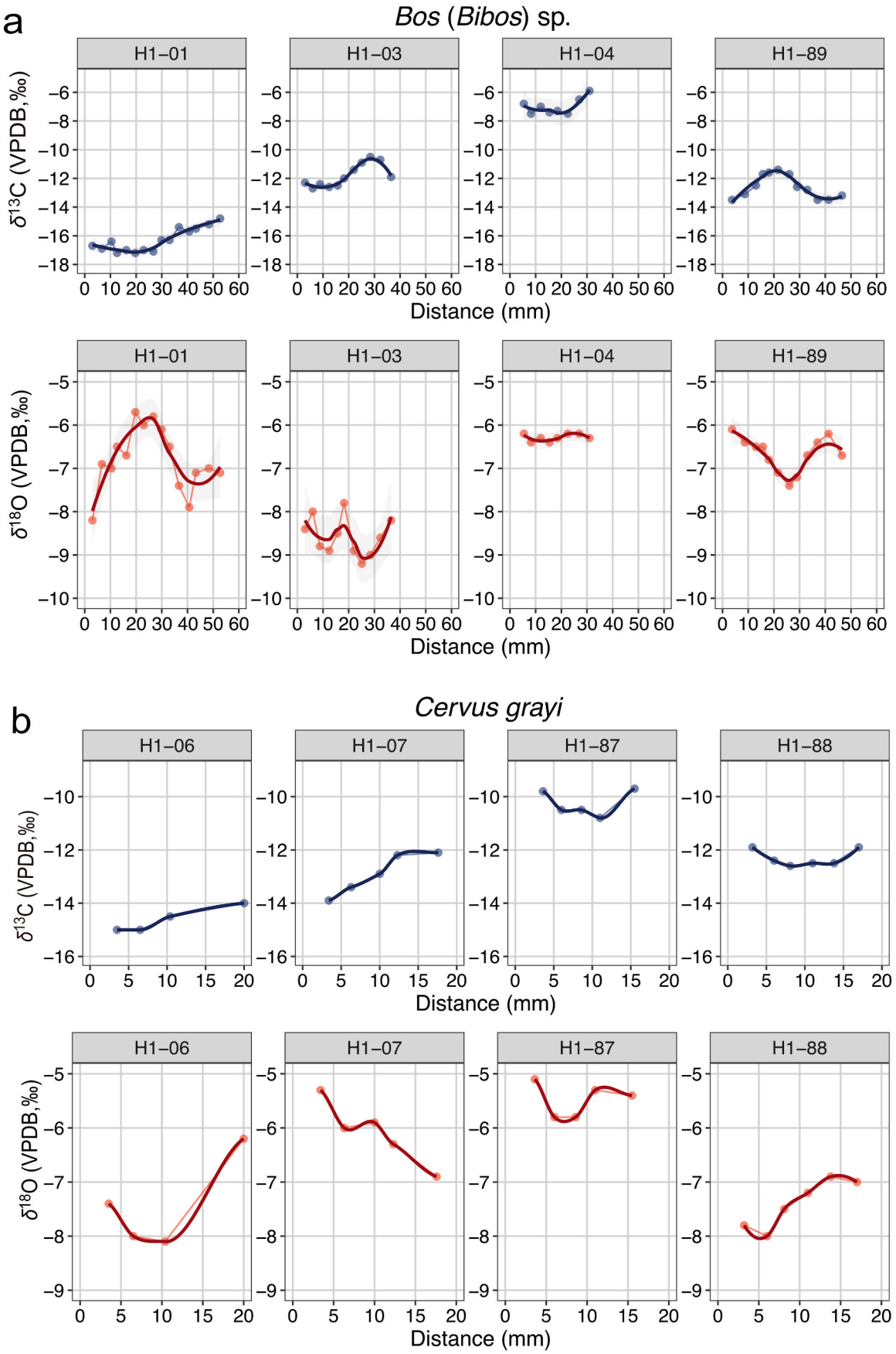

Fig. 3. Serial isotopic profiles of the *Bos* (*Bibos*) sp. (a) and *Cervus grayi* (b) specimens in this study.(Lines represent LOESS smooths (span = 0.75) with shaded areas indicating 95 % confidence intervals.).

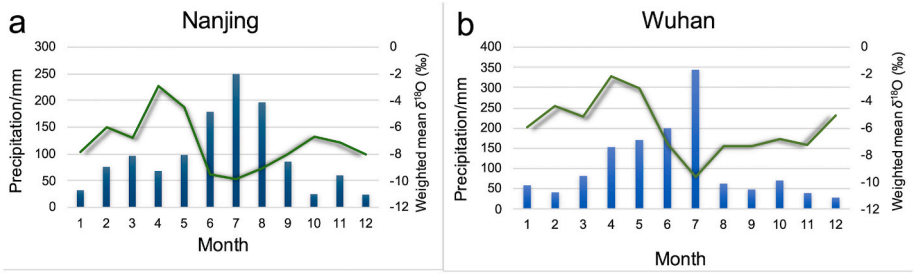

Fig. 4. Monthly precipitation and weighted mean $\delta^{18}O$ values in (a) Nanjing (1987–1992) and (b) Wuhan (1986–1998) (data were sourced from: https://nucleus.iaea.org/wiser/index.aspx).

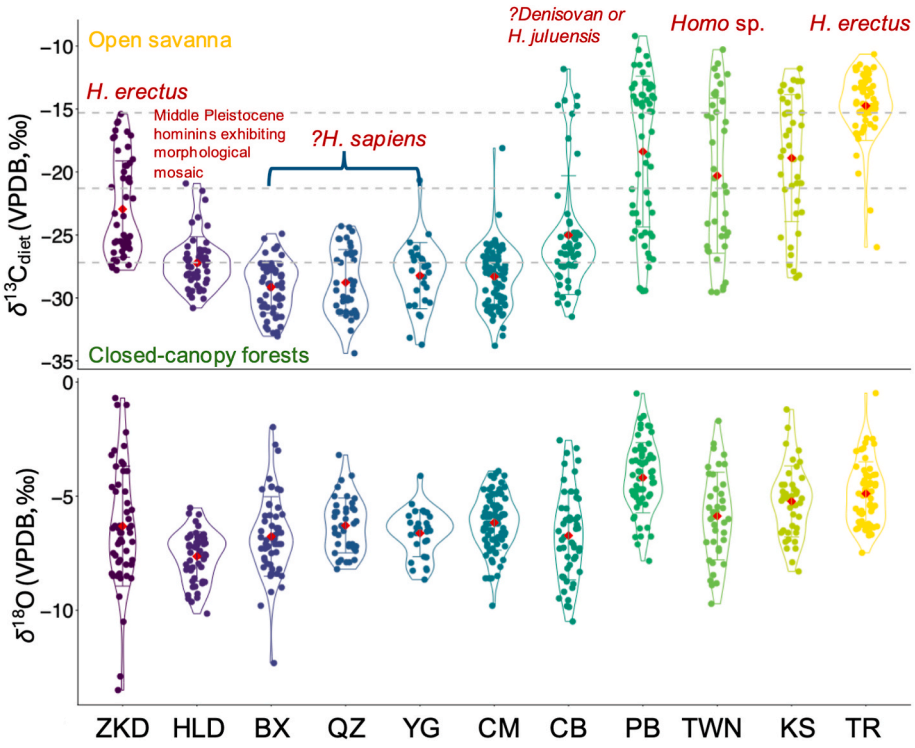

Fig. 5. $\delta^{13}C_{diet}$ and $\delta^{18}O$ values of eleven sites in eastern Asia during the Middle Pleistocene (774–129 ka) (Site abbreviations and their ages are as follows: Zhoukoudian (ZKD), ca. 720–470 ka; Hualongdong (HLD), 331–275 ka; Baxian Cave (BX), 200–143 ka; Quzai Cave (QZ), 214–187 ka; Yugongdong (YG), 252–200 ka; Coc Muoi (CM), 148–117 ka; Cobra Cave (CB), 164–131 ka; Pha Bong (PB), 400–200 ka; Tham Wiman Nakin (TWN), >169 ka; Khok Sung (KS), 217–130 ka; Trinil (TR), 540–430 ka). The raw data, comprising 563 isotopic values (derived from bulk samples for non-serially sampled teeth and from the mean of serial samples for serially sampled teeth), are provided in Table S2. Data resources are like the same as in Table 2. For the violin plots, the width of the "violin" at a particular value reflects the data density at that point. For the error bars, the red points are the mean values of each dataset, and the error bars indicate the standard deviations.). (For interpretation of the references to color in this figure legend, the reader is referred to the Web version of this article.)

2021) resembling those of Guangxi sites at the same latitude (Figs. 5 and 6; Tables 2 and 3, S3, S4), indicating an environment dominated by closed-canopy forests under warmer and more humid climatic conditions. Conversely, Cobra Cave (164–131 ka, Laos) exhibits broad $\delta^{13}C_{diet}$ variations (−25.0 ± 4.7 ‰, −31.5 ‰ to −11.8 ‰, n = 52), reflecting mixed forested-open landscapes (Bacon et al., 2023). Its $\delta^{13}C_{diet}$ values are significantly higher than Guangxi sites and Coc Muoi, suggesting a more open environment, potentially influenced by higher elevation (1116 m asl) (Bacon et al., 2023).

Three sites from Thailand display wide $\delta^{13}C_{diet}$ ranges (Pushkina et al., 2010; Bocherens et al., 2017; Suraprasit et al., 2018, 2020) without inter-site differences (Fig. 5, Table 2, S3). Their $\delta^{13}C_{diet}$ values are significantly higher than most other sites (Fig. 5, Table 2, S3), indicating the existence of the C_4 grasslands. Khok Sung (217 or 130 ka, Duval et al. (2019)) and Tham Wiman Nakin (>169 ka) may be partially contemporaneous, while Pha Bong dates to 400–200 ka based on faunal composition, mainly the presence of *Gigantopithecus* (Suraprasit et al., 2020). Furthermore, the distinct landscapes of Thailand, Vietnam, and Laos underscore the regional diversity within Mainland Southeast Asia.

The regional oxygen isotope data reveal statistically significant patterns that align with and enhance the dietary evidence from carbon isotopes. A distinct aridity cluster is evident, comprising the Thai sites (Pha Bong, −4.1 ± 1.5 ‰, n = 61; Khok Sung, −5.2 ± 1.6 ‰, n = 41; Tham Wiman Nakin, −5.9 ± 1.9 ‰, n = 39) and Javan Trinil (−4.9 ± 1.4 ‰, n = 55), which consistently exhibit the highest $\delta^{18}O$ values. This is coupled with their significantly high $\delta^{13}C_{diet}$ values, robustly indicating open, arid environments where intense evaporation and C_4 grassland expansion co-occurred (Fig. 5). Conversely, Hualongdong forms a distinct humid cluster, characterized by the region's lowest $\delta^{18}O$ values (−7.6 ± 1.1 ‰), alongside a clear C_3 dietary signal (Table 3, S4). The $\delta^{18}O$ differences between Hualongdong and other southern sites (mean $\delta^{18}O$ values of Guangxi sites, Coc Muoi, and Cobra Cave range

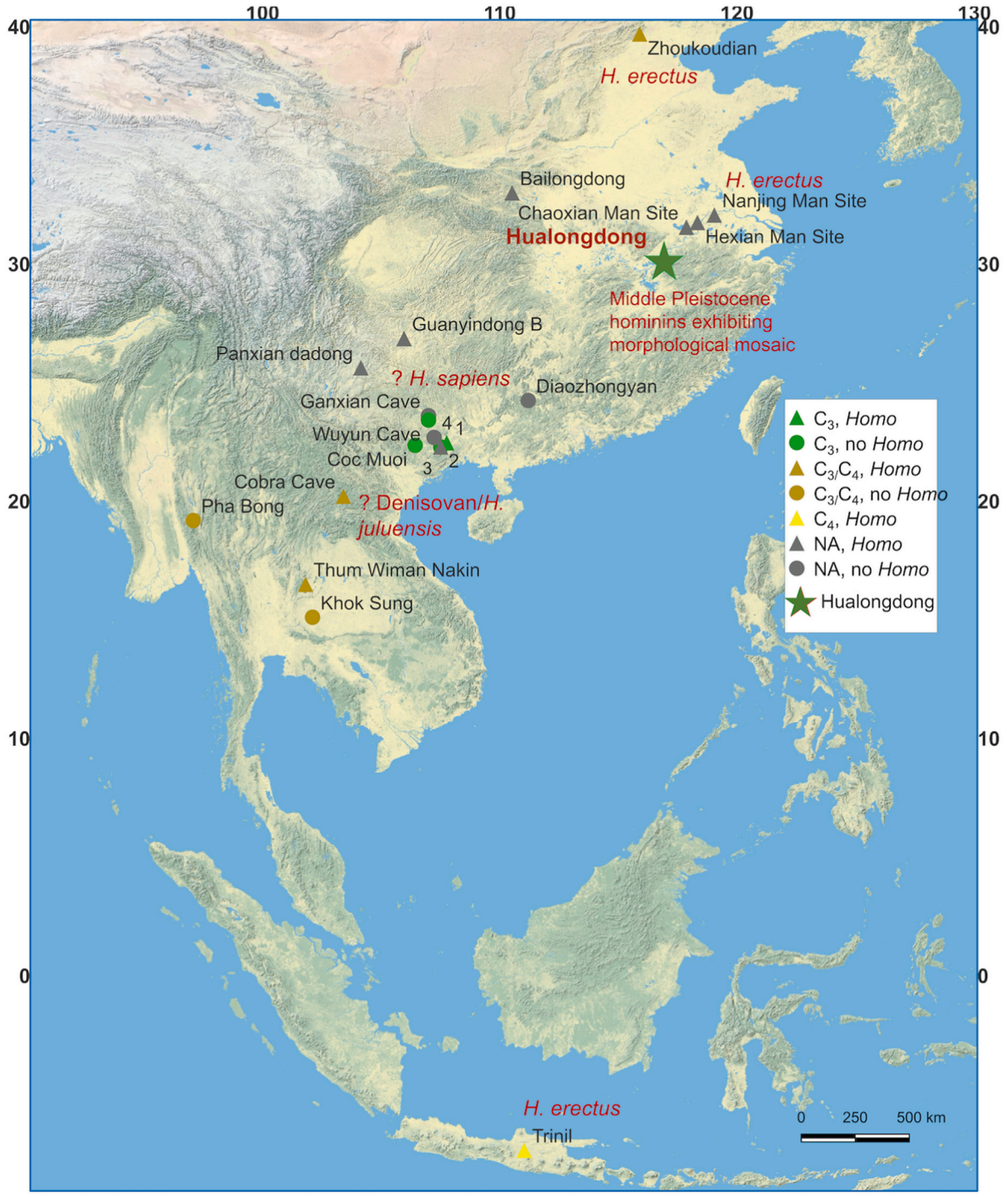

Fig. 6. Map of the Middle Pleistocene (774–129 ka) sites in eastern Asia The sites in the Chongzuo area of Guangxi province are marked with numbers. 1: Baxian Cave, Yugongdong, Quzai Cave; 2: Hejiang Cave; 3: Zhiren Cave; 4: Black Cave. The sites are depicted using different colors and symbols according to their ecological types, as inferred from $\delta^{13}C_{diet}$ values (Methods) and the presence of hominin fossils and/or artefacts (triangles indicate hominin presence while circles indicate absence). NA indicates the absence of carbon isotopic data. (For interpretation of the references to color in this figure legend, the reader is referred to the Web version of this article.)

from −6.8 ‰ to −6.2 ‰) likely reflect its higher latitude and cooler temperature, consistent with modern climate gradients (weather.cma.cn). The high variability of $\delta^{18}O$ values at Zhoukoudian remains consistent with its complex, long-term depositional history.

Among these eleven sites, serial isotopic data are available from Yugongdong, Baxian Cave, Hualongdong, and Khok Sung (Suraprasit et al., 2018; Ma et al., 2019b; Sun et al., 2019; this study), where different taxa were analyzed in these sites. Overall, annual $\delta^{13}C$ and $\delta^{18}O$ variations are limited (mean ranges <3 ‰), suggesting limited seasonality in subtropical Asia. Inverse $\delta^{13}C$-$\delta^{18}O$ relationships occur in 3 out of 7 Baxian, 5 out of 11 Yugongdong, and 4 out of 8 Hualongdong tooth specimens, indicating the influence of the EASM and the presence of seasonal C_4 plants as aforementioned (Biasatti et al., 2010; Ciner et al., 2015; Ma et al., 2023) (Table S5). The absence of this pattern at Khok Sung (n = 3) (Suraprasit et al., 2018) may reflect different precipitation regimes and vegetation dynamic in Thailand.

Overall, comparative analyses of mammalian enamel stable isotopes across eastern Asia during the Middle Pleistocene reveal distinct

Table 3
Pairwise comparisons of $\delta^{18}O$ values among Middle Pleistocene eastern Asian sites.

	Quzai Cave	Baxian Cave	Coc Muoi	Cobra Cave	Yugongdong	Hualongdong	Pha Bong	Tham Wiman Nakin	Khok Sung	Zhoukoudian
Baxian Cave										
Coc Muoi										
Cobra Cave										
Yugongdong										
Hualongdong	***		***		**					
Pha Bong	***	***	***	***	***	***				
Tham Wiman Nakin						***	**			
Khok Sung		***		*	*	***				
Zhoukoudian						*	***			
Trinil	***	***	***	***	***	***				*

Values represent adjusted *p*-values from Mann-Whitney *U* tests with Bonferroni correction. Significance levels: *p < 0.05, **p < 0.01, ***p < 0.001. Empty cells indicate non-significant differences (p ≥ 0.05). Complete pairwise *p*-values are provided in Supplementary Table S4. The references are the same with Table 2.

regional paleoenvironmental patterns: north China, east-central China, and southwestern China, as well as the distinct regions of mainland Southeast Asia and Java each exhibit unique ecological signatures. This broad paleoenvironmental heterogeneity across Middle Pleistocene eastern Asia is attributed to the combined effects of global climate fluctuations and regional factors, such as the East Asian Monsoon dynamics and complex topography. Notably, despite sharing the characteristic *Ailuropoda-Stegodon* faunal assemblage (Yijing Zhang et al., 2024), South China and Southeast Asia displayed remarkable paleoenvironmental complexity and diversity, highlighting ecological variability in subtropical eastern Asia and the need for stable isotope analyses for detailed paleoecological reconstruction.

5.2. Implication for hominin evolution in eastern Asia

The paleoenvironmental heterogeneity across Middle Pleistocene eastern Asia—encompassing C_3/C_4 mixed woodlands in North China, closed-canopy forests in South China, fragmented forests and grasslands in mainland Southeast Asia, and arid savannas in Java—provides a critical ecological framework for interpreting coeval hominin distribution, adaptation, and evolution. Middle Pleistocene hominins in eastern Asia occupied remarkably diverse settings, from closed forests to open grasslands, a pattern that aligns with evidence for hominin adaptive radiation into diverse biomes (Zeller et al., 2023; Foister et al., 2024). While large-scale paleoenvironmental analyses have thoroughly explored links between Middle Pleistocene climatic variability and hominin diversity (Ao et al., 2020), this study offers direct mammalian faunal isotopic evidence together with hominin-related remains to refine these relationships.

Among the analyzed sites, Zhoukoudian (north China) and Trinil (Java) yield definitive *H. erectus* fossils associated with mixed C_3/C_4 vegetation (Gaboardi et al., 2005; Janssen et al., 2016; Puspaningrum et al., 2020). Although these landscapes differed ecologically from their African counterparts, where C_4 grassland often dominates (Bocherens et al., 1996; Cerling et al., 2013), their structural openness may have served as ecological templates facilitating population occupation and dispersal.

Of the nine sites in subtropical eastern Asia analyzed, six potentially preserve hominin fossils, though only Hualongdong and Cobra Cave have formally published fossil records. Cobra Cave (northern Laos, 164–131 ka) exhibits higher $\delta^{13}C_{diet}$ values than sites in China and Vietnam, indicating more open environments. A Denisovan molar from this site (Demeter et al., 2022), alternatively attributed to *H. juluensis* (Bae and Wu, 2024), exhibits a $\delta^{13}C$ value consistent with exploitation of open habitats (Bacon et al., 2023). A tooth of *Homo* sp. has also been recovered from Tham Wiman Nakin alongside the mammal assemblage, though its significance remains underexplored (Tougard et al., 1998; Bae, 2010). Notably, while no definitive hominin fossils have been identified at the Middle Pleistocene Thai sites, their open environmental settings suggest that such open landscapes may have served as a potential corridor for hominin migration.

In southern China, hominin fossils from three Guangxi sites—Yugongdong (252–200 ka), Quzai Cave (214–187 ka), Baxian Cave (200–143 ka)—have been tentatively attributed to *H. sapiens* in preliminary reports (Dong et al., 2014; Ma et al., 2019a; Sun et al., 2019). Pending full publication of these materials, the region offers robust evidence from other, well-documented sites for the presence of early modern humans. Notably, Zhiren Cave (or *H. sapiens* Cave, 110 ka or 190–130 ka) preserves the earliest modern human fossils with derived morphological traits (Jin et al., 2009; Liu et al., 2010; Ge et al., 2020), and Daoxian has yielded 47 *H. sapiens* teeth with fully modern morphology dated to 80–120 ka (Liu et al., 2015). Although direct isotopic data are unavailable for Zhiren Cave and Daoxian, the C_3-dominated $\delta^{13}C_{diet}$ values from the Guangxi sites may provide insights into the closed-canopy forested environments of southern China during the late Middle to early Late Pleistocene. This ecological context could imply an early capacity for adaptation to forested habitats among the human populations of this region.

Hualongdong has yielded over 50 human fossil elements, including the Hualongdong 6 adolescent skull and mandible, cranial pieces, isolated teeth, and femoral diaphyseal sections (Wu et al., 2019, 2021, 2025; Xing et al., 2021). Morphological analyses reveal mosaic features: the second molar and the frontal bone retain traits common in *H. erectus*, while the femoral elements exhibit a combination of archaic and derived characteristics (Liu and Wu, 2025). This morphological diversity underscores Hualongdong's complex position in the hominin record. The lithic assemblage at Hualongdong is characterized as a low-investment Mode 1 core-and-flake industry, utilizing locally available chert and quartz (Wu et al., 2019; Pei et al., 2025). This technology aligns with a subsistence economy focused on animal resources, as evidenced by cut marks on astragali of cervids and bovids confirming the processing of carcasses (S. Liu et al., 2025) and mortality profiles of large bovids suggesting flexible hunting strategies (including potentially ambush and endurance, with a possible focus on juvenile individuals) (B. Liu et al., 2025). Combined with the $\delta^{13}C_{diet}$ values of these prey species in this study (cervids and bovids, range: −30.8 ‰ to −21.5 ‰, mean −26.6 ± 2.5 ‰, n = 17), these lines of evidence indicate that hominins exploited mammalian resources from diverse environments. Together, the archaeological, taphonomic, and isotopic data outline a coherent suite of behavioral adaptations to the mosaic environment.

The significance of Hualongdong extends beyond the site itself, providing a key to interpreting the broader paleoecological context of hominin occupation in east-central China. This region, lacking major geographic barriers, is recognized as a corridor for faunal and hominin migrations (Norton and Braun, 2011; Ma et al., 2021). Hominin fossils have been recovered from other sites near 30°N (Fig. 6), including *H. erectus* from the Nanjing Man site (620–580 ka) and Hexian (ca. 412 ka), as well as Middle Pleistocene hominins with more derived

morphological traits from Chaoxian (300–200 ka) and Hualongdong (331–275 ka) (Xu et al., 1984; The Tangshan Archaeological Team from Nanjing Municipal Museum and Archaeology Department of Peking University, 1996; Zheng and Huang, 2001; Liu et al., 2005, 2017, 2022; Kong, 2018; Wu et al., 2019). Critically, these sites share a similar faunal composition, characterized by a mix of the classic *Ailuropoda-Stegodon* assemblages and Palearctic genera (e.g., *Sinomegaceros, Elaphurus, Equus,* and *Capreolus*) (Xu et al., 1984; Zheng and Huang, 2001; Wu et al., 2002; Tong et al., 2018, 2019, 2025).

However, paleoenvironmental data for these sites have remained limited. As the only location in this region with detailed isotopic reconstructions (Fig. 6), Hualongdong serves as a critical benchmark, providing the first insight into the mosaic habitats that likely prevailed in east-central China. It strongly suggests that contemporaneous sites in Anhui and Jiangsu provinces below 500 m altitude were likely dominated by forest mosaic environments. Nevertheless, additional isotopic and paleoenvironmental studies at other sites are needed to test and refine this reconstruction. Despite chronological and contextual differences, diverse hominins in this region appear to have occupied comparable mosaic habitats. Within these settings, although direct isotopic evidence from hominins is needed to clarify their specific dietary composition, this ecosystem would have offered a spectrum of resources: closed-canopy environments would have provided stable, protected resources, while the seasonally dynamic woodlands with C_4 vegetation likely facilitated mobility and offered alternative foraging opportunities.

Recent studies have highlighted the morphological and taxonomic complexity of hominins in the late Middle Pleistocene of East Asia (Chen et al., 2019; Ni et al., 2021; Bae and Wu, 2024; Fu et al., 2025; Tsutaya et al., 2025). Within this context, the Hualongdong hominins are distinguished by a mosaic of features that includes several derived traits, giving them a closer morphological resemblance to *H. sapiens* than that observed in other contemporary populations. This is significant given previous hypotheses suggesting that only *H. sapiens* could adapt to dense forest habitats (Fleagle et al., 2010; Roberts and Petraglia, 2015). This finding challenges earlier hypotheses that attributed the absence of archaic hominins at sites such as Coc Muoi to rainforests acting as ecological barriers (Bacon et al., 2021).

Against this backdrop, the Hualongdong hominins inhabited a mosaic environment that was slightly more open than the contemporaneous rainforests of Guangxi yet distinct from the more open habitats often associated with *H. erectus*. This suggests a broader habitat tolerance range among Middle Pleistocene hominins. Populations exhibiting more derived morphologies were successfully exploiting these forest-woodland ecotones in east-central China. The unique environmental context of Hualongdong may thus represent a key driver underlying the regional evolutionary variability, potentially contributing to the distinctive morphological patterns observed at the site. Notably, their successful persistence in this forest mosaic provides critical insights into behavioral traits that may have facilitated the adaptation of later hominins to tropical ecosystems. Further investigation into their material culture will clarify the depth of their adaptive strategies, potentially bridging key gaps in our understanding of how hominin behavioral plasticity contributed to the evolutionary pathways that eventually led to modern human ecological success.

6. Conclusion

Through stable isotopic analyses of mammalian remains from Hualongdong, this study reconstructs the paleoenvironmental context for late Middle Pleistocene (331–275 ka) hominins in east-central China. The ecological settings at Hualongdong were characterized by a C_3-dominated forest ecosystem with year-round C_4 grass presence, forming a mosaic of dense forests and woodlands shaped by the EASM. This mosaic landscape would have provided stable resources through closed-canopy forests and favorable conditions for habitation and migration via seasonally dynamic intermediate woodlands with localized C_4 vegetation.

Comparative isotopic analyses across China and Southeast Asia highlight significant paleoenvironmental heterogeneity during the Middle Pleistocene, revealing diverse ecosystems ranging from C_3/C_4 mixed woodlands in northern China, to forest mosaics in east-central China (as represented by Hualongdong), to closed-canopy forests in southwestern China, and to arid savannas in Java. Within this broader environmental framework, Hualongdong represents a key transitional zone. Its mosaic of forests and open woodlands, distinct from the more open habitats of northern China and the denser forests of southwestern China, reflects an intermediate stage in hominin ecological adaptation, connecting earlier specialization in open environments and the subsequent colonization of closed forests.

Notably, Hualongdong hominins, inhabiting a forest-woodland mosaic, exhibit a notable mosaic of archaic and derived traits, reflecting adaptations that differ from both typical *H. erectus* and other contemporaneous populations. Their persistence in this mosaic environment underscores the development of behavioral flexibility, providing insights into how Middle Pleistocene hominins respond to increasingly diverse forest ecosystems across eastern Asia. This study thus enhances our understanding of the interplay between paleoenvironmental dynamics and hominin adaptive strategies, highlighting east-central China's significance as an ecological crossroads in Middle Pleistocene hominin evolution. Future investigations into lithic technologies and hominin behavioral traces at Hualongdong will further clarify the nature of these adaptive developments.

Author contributions

Jiao Ma: Conceptualization, Data curation, Funding acquisition, Investigation, Methodology, Software, Visualization, Roles/Writing - original draft, Writing - review & editing. Wu Liu, Xiujie Wu: Conceptualization; Resources; Writing - review & editing; Hervé Bocherens: Conceptualization; Writing - review & editing; Haowen Tong, Shuwen Pei: Resources, Writing - review & editing.

Declaration of competing interest

The authors declare that they have no known competing financial interests or personal relationships that could have appeared to influence the work reported in this paper.

Acknowledgements

We sincerely thank the three anonymous reviewers for their constructive suggestions, which have significantly improved the quality of this manuscript. We thank H.W. Li and H.Y. Rao for their help in the lab. We thank T. Deng and Q. Li for their insightful discussions. We also acknowledge the valuable assistance provided by AI assistants (DeepSeek, Geogpt, Doubao) in language polishing and grammar checking. This work was supported by the National Key Research and Development Program of China (2023YFF0804501) and Youth Innovation Promotion (2022070).

Appendix A. Supplementary data

Supplementary data to this article can be found online at https://doi.org/10.1016/j.quascirev.2025.109746.

Data availability

All data and/or code is contained within the submission.

References

Ahrestani, F.S., Heitkönig, I.M.A., Matsubayashi, H., Prins, H.H.T., 2016. Grazing and browsing by large herbivores in South and Southeast Asia. In: Ahrestani, F.S., Sankaran, M. (Eds.), The Ecology of Large Herbivores in South and Southeast Asia. Springer, Netherlands, Dordrecht, pp. 99–120.

Ambrose, S.H., Butler, B.M., Hanson, D.B., Hunter-Anderson, R.L., Krueger, H.W., 1997. Stable isotopic analysis of human diet in the Marianas Archipelago, Western Pacific. Am. J. Phys. Anthropol. 104, 343–361.

Ao, H., Rohling, E.J., Stringer, C., Roberts, A.P., Dekkers, M.J., Dupont-Nivet, G., Yu, J., Liu, Q., Zhang, P., Liu, Z., Ma, X., Zhou, W., Jin, Z., Xiao, G., Wang, H., Sun, Q., Yang, P., Peng, X., Shi, Z., Qiang, X., An, Z., 2020. Two-stage mid-brunhes climate transition and mid-pleistocene human diversification. Earth Sci. Rev. 210, 103354.

Bacon, A., Bourgon, N., Welker, F., Cappellini, E., Fiorillo, D., Tombret, O., Huong, N.T. M., Tuan, N.A., Sayavonkhamdy, T., Souksavatdy, V., Sichanthongtip, P., Antoine, P., Duringer, P., Ponche, J., Westaway, K., Joannes-Boyau, R., Boesch, Q., Suzzoni, E., Frangeul, S., Patole-Edoumba, E., Zachwieja, A., Shackelford, L., Demeter, F., Hublin, J., Dufour, É., 2021. A multi-proxy approach to exploring *Homo sapiens*' arrival, environments and adaptations in Southeast Asia. Sci. Rep. 11, 21080.

Bacon, A., Bourgon, N., Dufour, E., Demeter, F., Zanolli, C., Westaway, K.E., Joannes-Boyau, R., Duringer, P., Ponche, J., Morley, M.W., Suzzoni, E., Frangeul, S., Boesch, Q., Antoine, P., Boualaphane, S., Sichanthongtip, P., Sihanam, D., Huong, N. T.M., Tuan, N.A., Fiorillo, D., Tombret, O., Patole-Edoumba, E., Zachwieja, A., Luangkhoth, T., Souksavatdy, V., Dunn, T.E., Shackelford, L., Hublin, J., 2023. Palaeoenvironments and hominin evolutionary dynamics in southeast Asia. Sci. Rep. 13, 16165.

Bae, C.J., 2010. The late Middle Pleistocene hominin fossil record of eastern Asia: synthesis and review. Am. J. Phys. Anthropol. 143, 75–93.

Bae, C.J., Wu, X., 2024. Making sense of eastern Asian Late Quaternary hominin variability. Nat. Commun. 15, 9479.

Balasse, M., 2002. Reconstructing dietary and environmental history from enamel isotopic analysis: time resolution of intra-tooth sequential sampling. Int. J. Osteoarchaeol. 12, 155–165.

Bender, M.M., 1968. Mass spectrometric studies of carbon 13 variations in corn and other grasses. Radiocarbon 10, 468–472.

Biasatti, D., Wang, Y., Deng, T., 2010. Strengthening of the East Asian summer monsoon revealed by a shift in seasonal patterns in diet and climate after 2–3 Ma in northwest China. Palaeogeogr. Palaeoclimatol. Palaeoecol. 297, 12–25.

Blumenthal, S.A., Cerling, T.E., Chritz, K.L., Bromage, T.G., Kozdon, R., Valley, J.W., 2014. Stable isotope time-series in mammalian teeth: *in situ* $\delta^{18}O$ from the innermost enamel layer. Geochem. Cosmochim. Acta 124, 223–236.

Bocherens, H., Koch, P.L., Mariotti, A., Geraads, D., Jaeger, J.J., 1996. Isotopic biogeochemistry (^{13}C, ^{18}O) of mammalian enamel from African Pleistocene Hominid sites. Palaios 11, 306–318.

Bocherens, H., Schrenk, F., Chaimanee, Y., Kullmer, O., Mörike, D., Pushkina, D., Jaeger, J.J., 2017. Flexibility of diet and habitat in Pleistocene South Asian mammals: implications for the fate of the giant fossil ape *Gigantopithecus*. Quat. Int. 434, 148–155.

Bryant, J.D., Froelich, P.N., 1995. A model of oxygen isotope fractionation in body water of large mammals. Geochem. Cosmochim. Acta 59, 4523–4537.

Cai, Y., Pei, S., Jin, Z., 2025. Sedimentary feature and chronology of Hualongdong site in Dongzhi, Anhui Province. Acta Anthropol. Sin. 44, 742–753 (in Chinese with English abstract).

Cerling, T.E., Harris, J.M., 1999. Carbon isotope fractionation between diet and bioapatite in ungulate mammals and implications for ecological and paleoecological studies. Oecologia 120, 347–363.

Cerling, T.E., Manthi, F.K., Mbua, E.N., Leakey, L.N., Leakey, M.G., Leakey, R.E., Brown, F.H., Grine, F.E., Hart, J.A., Kaleme, P., Roche, H., Uno, K.T., Wood, B.A., 2013. Stable isotope-based diet reconstructions of Turkana Basin hominins. Proc. Natl. Acad. Sci. 110, 10501–10506.

Cerling, T.E., Bernasconi, S.M., Hofstetter, L.S., Jaggi, M., Wyss, F., Rudolf von Rohr, C., Clauss, M., 2021. CH_4/CO_2 ratios and carbon isotope enrichment between diet and breath in herbivorous mammals. Front. Ecol. Evol. 9, 638568.

Chen, F., Welker, F., Shen, C.C., Bailey, S.E., Bergmann, I., Davis, S., Xia, H., Wang, H., Fischer, R., Freidline, S.E., Yu, T.L., Skinner, M.M., Stelzer, S., Dong, Guangrong, Fu, Q., Dong, Guanghui, Wang, J., Zhang, D., Hublin, J.J., 2019. A late Middle Pleistocene Denisovan mandible from the Tibetan Plateau. Nature 569, 409–412.

Ciner, B., Wang, Y., Deng, T., Flynn, L., Hou, S., Wu, W., 2015. Stable carbon and oxygen isotopic evidence for Late Cenozoic environmental change in Northern China. Palaeogeogr. Palaeoclimatol. Palaeoecol. 440, 750–762.

Clementz, M.T., Fox-Dobbs, K., Wheatley, P.V., Koch, P.L., Doak, D.F., 2009. Revisiting old bones: coupled carbon isotope analysis of bioapatite and collagen as an ecological and palaeoecological tool. Geol. J. 44, 605–620.

The Tangshan Archaeological Team from Nanjing Municipal Museum, Archaeology Department of Peking University, 1996. Locality of the Nanjing Man Fossils (1993-1994). Culture Relics Pressing House, Beijing. (in Chinese with English abstract).

Demeter, F., Zanolli, C., Westaway, K.E., Joannes-Boyau, R., Duringer, P., Morley, M.W., Welker, F., Rüther, P.L., Skinner, M.M., McColl, H., Gaunitz, C., Vinner, L., Dunn, T. E., Olsen, J.V., Sikora, M., Ponche, J.L., Suzzoni, E., Frangeul, S., Boesch, Q., Antoine, P.O., Pan, L., Xing, S., Zhao, J.X., Bailey, R.M., Boualaphane, S., Sichanthongtip, P., Sihanam, D., Patole-Edoumba, E., Aubaile, F., Crozier, F., Bourgon, N., Zachwieja, A., Luangkhoth, T., Souksavatdy, V., Sayavongkhamdy, T., Cappellini, E., Bacon, A.M., Hublin, J.J., Willerslev, E., Shackelford, L., 2022. A Middle Pleistocene Denisovan molar from the Annamite chain of northern Laos. Nat. Commun. 13, 2557.

Dong, W., Wang, Y., Jin, C., Qin, D., Xu, Q., Zhang, L., 2014. Artiodactyla associated with *Homo sapiens* from Gongjishan, Chongzuo, Guangxi, South China. Acta Anthropol. Sin. 33, 355–368 (in Chinese with English abstract).

Dutton, A., Wilkinson, B.H., Welker, J.M., Bowen, G.J., Lohmann, K.C., 2005. Spatial distribution and seasonal variation in $^{18}O/^{16}O$ of modern precipitation and river water across the conterminous USA. Hydrol. Process. 19, 4121–4146.

Duval, M., Fang, F., Suraprasit, K., Jaeger, J.-J., Benammi, M., Chaimanee, Y., Cibanal, J. I., Grün, R., 2019. Direct ESR dating of the Pleistocene vertebrate assemblage from Khok Sung locality, Nakhon Ratchasima Province, Northeast Thailand. Palaeontol. Electron. 22.3.69, 1–25.

Farquhar, G.D., Ehleringer, J.R., Hubick, K.T., 1989. Carbon isotope discrimination and photosynthesis. Annu. Rev. Plant Biol. 40, 503–537.

Fleagle, J.G., Shea, J.J., Grine, F.E., Baden, A.L., Leakey, R.E. (Eds.), 2010. Out of Africa I, Vertebrate Paleobiology and Paleoanthropology. Springer, Netherlands, Dordrecht.

Foerster, V., Asrat, A., Bronk Ramsey, C., Brown, E.T., Chapot, M.S., Deino, A., Duesing, W., Grove, M., Hahn, A., Junginger, A., Kaboth-Bahr, S., Lane, C.S., Opitz, S., Noren, A., Roberts, H.M., Stockhecke, M., Tiedemann, R., Vidal, C.M., Vogelsang, R., Cohen, A.S., Lamb, H.F., Schaebitz, F., Trauth, M.H., 2022. Pleistocene climate variability in eastern Africa influenced hominin evolution. Nat. Geosci. 15, 805–811.

Foister, T.I.F., Liu, L., Saarinen, J., Tallavaara, M., Zhang, H., Žliobaitė, I., 2024. Quantifying heterogeneity of hominin environments in and out of Africa using herbivore dental traits. Quat. Sci. Rev. 337, 108791.

Fricke, H.C., O'Neil, J.R., 1996. Inter-and intra-tooth variation in the oxygen isotope composition of mammalian tooth enamel phosphate: implications for palaeoclimatological and palaeobiological research. Palaeogeogr. Palaeoclimatol. Palaeoecol. 126, 91–99.

Fu, Q., Cao, P., Dai, Q., Bennett, E.A., Feng, X., Yang, M.A., Ping, W., Pääbo, S., Ji, Q., 2025. Denisovan mitochondrial DNA from dental calculus of the >146,000-year-old Harbin cranium. Cell 188, 1–8.

Gaboardi, M., Deng, T., Wang, Y., 2005. Middle Pleistocene climate and habitat change at Zhoukoudian, China, from the carbon and oxygen isotopic record from herbivore tooth enamel. Quat. Res. 63, 329–338.

Ge, J., Deng, C., Wang, Y., Shao, Q., Zhou, X., Xing, S., Pang, H., Jin, C., 2020. Climate-influenced cave deposition and human occupation during the Pleistocene in Zhiren Cave, southwest China. Quat. Int. 559, 14–23.

Gosling, W.D., Scerri, E.M.L., Kaboth-Bahr, S., 2022. The climate and vegetation backdrop to hominin evolution in Africa. Philos. Trans. R. Soc. B Biol. Sci. 377, 20200483.

Green, D.R., Smith, T.M., Green, G.M., Bidlack, F.B., Tafforeau, P., Colman, A.S., 2018. Quantitative reconstruction of seasonality from stable isotopes in teeth. Geochem. Cosmochim. Acta 235, 483–504.

Han, H., Wei, W., Nie, Y., Zhou, W., Hu, Y., Wu, Q., Wei, F., 2016. Distinctive diet-tissue isotopic discrimination factors derived from the exclusive bamboo-eating giant panda. Integr. Zool. 11, 447–456.

Harvati, K., Röding, C., Bosman, A.M., Karakostis, F.A., Grün, R., Stringer, C., Karkanas, P., Thompson, N.C., Koutoulidis, V., Moulopoulos, L.A., Gorgoulis, V.G., Kouloukoussa, M., 2019. Apidima Cave fossils provide earliest evidence of *Homo sapiens* in Eurasia. Nature 571, 500–504.

Hemami, M.R., Watkinson, A.R., Dolman, P.M., 2004. Habitat selection by sympatric muntjac (*Muntiacus reevesi*) and roe deer (*Capreolus capreolus*) in a lowland commercial pine forest. For. Ecol. Manag. 194, 49–60.

Hershkovitz, I., Weber, G.W., Quam, R., Duval, M., Grün, R., Kinsley, L., Ayalon, A., Bar-Matthews, M., Valladas, H., Mercier, N., Arsuaga, J.L., Martinón-Torres, M., Bermúdez de Castro, J.M., Fornai, C., Martín-Francés, L., Sarig, R., May, H., Krenn, V.A., Slon, V., Rodríguez, L., García, R., Lorenzo, C., Carretero, J.M., Frumkin, A., Shahack-Gross, R., Bar-Yosef Mayer, D.E., Cui, Y., Wu, X., Peled, N., Groman-Yaroslavski, I., Weissbrod, L., Yeshurun, R., Tsatskin, A., Zaidner, Y., Weinstein-Evron, M., 2018. The earliest modern humans outside Africa. Science 359, 456–459.

Higgins, P., MacFadden, B.J., 2004. "Amount Effect" recorded in oxygen isotopes of late glacial horse (*Equus*) and bison (*Bison*) teeth from the Sonoran and Chihuahuan deserts, southwestern United States. Palaeogeogr. Palaeoclimatol. Palaeoecol. 206, 337–353.

Hillson, S., 2005. Teeth. Cambridge university press, Cambridge.

Janssen, R., Joordens, J.C.A., Koutamanis, D.S., Puspaningrum, M.R., de Vos, J., van der Lubbe, J.H.J.L., Reijmer, J.J.G., Hampe, O., Vonhof, H.B., 2016. Tooth enamel stable isotopes of Holocene and Pleistocene fossil fauna reveal glacial and interglacial paleoenvironments of hominins in Indonesia. Quat. Sci. Rev. 144, 145–154.

Jiang, Q., Zhao, L., Hu, Y., 2020. Isotopic (C, O) variations of fossil enamel bioapatite caused by different preparation and measurement protocols: a case study of *Gigantopithecus* fauna. Vertebr. Palasiat. 58, 159–168.

Jiang, Q., Zhao, L., Guo, L., Hu, Y., 2021. First direct evidence of conservative foraging ecology of early *Gigantopithecus blacki* (~2 Ma) in Guangxi, southern China. Am. J. Phys. Anthropol. 176, 93–108.

Jiangzuo, Q., Liu, B., Liu, S., He, L., Tong, H., 2025. Fossil carnivora from the Hualongdong Site Loc.1 and their chronological and paleoenvironmental implications. Acta Anthropologica Sinica 44, 836–849 (in Chinese with English abstract).

Jin, C., Pan, W., Zhang, Y., Cai, Y., Xu, Q., Tang, Z., Wang, W., Wang, Y., Liu, J., Qin, D., 2009. The *Homo sapiens* Cave hominin site of Mulan Mountain, Jiangzhou District, Chongzuo, Guangxi with emphasis on its age. Chin. Sci. Bull. 54, 3848.

Joordens, J.C., d'Errico, F., Wesselingh, F.P., Munro, S., De Vos, J., Wallinga, J., Ankjærgaard, C., Reimann, T., Wijbrans, J.R., Kuiper, K.F., 2015. *Homo erectus* at Trinil on Java used shells for tool production and engraving. Nature 518, 228–231.

Kassambara, A., 2020. *ggpubr*: "*ggplot2*" Based Publication Ready Plots (R Package Version 0.4.0).
Koch, P.L., Fisher, D.C., Dettman, D., 1989. Oxygen isotope variation in the tusks of extinct proboscideans: a measure of season of death and seasonality. Geology 17, 515–519.
Kohn, M.J., 2010. Carbon isotope compositions of terrestrial C_3 plants as indicators of (paleo) ecology and (paleo) climate. Proc. Natl. Acad. Sci. 107, 19691–19695.
Kohn, M.J., Cerling, T.E., 2002. Stable isotope compositions of biological apatite. Rev. Mineral. Geochem. 48, 455–488.
Kohn, M.J., Schoeninger, M.J., Valley, J.W., 1996. Herbivore tooth oxygen isotope compositions: effects of diet and physiology. Geochem. Cosmochim. Acta 60, 3889–3896.
Kohn, M.J., Schoeninger, M.J., Valley, J.W., 1998. Variability in oxygen isotope compositions of herbivore teeth: reflections of seasonality or developmental physiology? Chem. Geol. 152, 97–112.
Kong, Y., 2018. Magnetostratigraphic dating of the hominin occupation of Bailong Cave, central China. Sci. Rep. 8, 9699.
Li, D., Hu, C., Wang, W., Chen, J., Tian, F., Huang, S., Bae, C.J., 2017. The stable isotope record in cervid tooth enamel from Tantang Cave, Guangxi: implications for the Quaternary East Asian monsoon. Quat. Int. 434, 156–162.
Liu, W., Wu, X., 2025. The hominin fossils from Hualongdong and their significance on human evolution. Acta Anthropol. Sin. 44, 727–741 (in Chinese with English abstract).
Liu, W., Zhang, Y., Wu, X., 2005. Middle Pleistocene human cranium from Tangshan (Nanjing), Southeast China: a new reconstruction and comparisons with *Homo erectus* from Eurasia and Africa. Am. J. Phys. Anthropol. 127, 253–262.
Liu, W., Jin, C.Z., Zhang, Y.Q., Cai, Y.J., Xing, S., Wu, X.J., Cheng, H., Edwards, R.L., Pan, W.S., Qin, D.G., An, Z.S., Trinkaus, E., Wu, X.Z., 2010. Human remains from Zhirendong, South China, and modern human emergence in East Asia. Proc. Natl. Acad. Sci. 107, 19201–19206.
Liu, W., Martinón-Torres, M., Cai, Y., Xing, S., Tong, H., Pei, S., Sier, M.J., Wu, Xiaohong, Edwards, R.L., Cheng, H., Li, Y., Yang, X., de Castro, J.M.B., Wu, Xiu-jie, 2015. The earliest unequivocally modern humans in southern China. Nature 526, 696–699. https://doi.org/10.1038/nature15696.
Liu, W., Martinón-Torres, M., Kaifu, Y., Wu, X., Kono, R.T., Chang, C.H., Wei, P., Xing, S., Huang, W., Bermúdez de Castro, J.M., 2017. A mandible from the Middle Pleistocene Hexian site and its significance in relation to the variability of Asian *Homo erectus*. Am. J. Phys. Anthropol. 162, 715–731.
Liu, W., Athreya, S., Xing, S., Wu, X., 2022. Hominin evolution and diversity: a comparison of earlier-Middle and later-Middle Pleistocene hominin fossil variation in China. Philos. Trans. R. Soc. B Biol. Sci. 377, 20210040.
Liu, B., Liu, S., Jin, Z., Deng, G., Wu, X., 2025. Hunting behavior of Hualongdong Hominid based on the teeth of gaur. Acta Anthropol. Sin. 44, 862–873 (in Chinese with English abstract).
Liu, S., Liu, B., Jin, Z., Deng, G., Tong, H., Wu, X., 2025. Mammalian astragalus fossils excavated at Hualongdong site. Acta Anthropol. Sin. 44, 816–835 (in Chinese with English abstract).
Louys, J., 2008. Quaternary extinctions in Southeast Asia. In: Mass Extinction. Springer Berlin Heidelberg, Berlin, Heidelberg, pp. 159–189.
Louys, J., Roberts, P., 2020. Environmental drivers of megafauna and hominin extinction in Southeast Asia. Nature 586, 402–406.
Ma, J., Wang, Y., Jin, C., Yan, Y., Qu, Y., Hu, Y., 2017. Isotopic evidence of foraging ecology of Asian elephant (*Elephas maximus*) in South China during the Late Pleistocene. Quat. Int. 443, 160–167.
Ma, J., Wang, Y., Jin, C., Hu, Y., Bocherens, H., 2019. Ecological flexibility and differential survival of Pleistocene *Stegodon orientalis* and *Elephas maximus* in mainland southeast Asia revealed by stable isotope (C, O) analysis. Quat. Sci. Rev. 212, 33–44.
Ma, J., Wang, Y., Jin, C.Z., Zhang, H.W., Hu, Y.W., 2019. A preliminary study of serial stable isotope analysis tracks foraging ecology of fossil Asian elephants in South China. Vertebr. Palasiat. 57, 225–240.
Ma, J., Wang, Y., Baryshnikov, G.F., Drucker, D.G., McGrath, K., Zhang, H., Bocherens, H., Hu, Y., 2021. The *Mammuthus-Coelodonta* Faunal complex at its southeastern limit: a biogeochemical paleoecology investigation in Northeast Asia. Quat. Int. 591, 93–106.
Ma, J., Sun, B., Bocherens, H., Deng, T., 2023. Dietary niche reconstruction of Pliocene and Pleistocene Equidae from the Linxia Basin of northwestern China based on stable isotope analysis. Palaeogeogr. Palaeoclimatol. Palaeoecol. 614, 111416.
Ma, J., Wang, S., Deng, T., 2024. When the woolly rhinoceroses roamed East Asia: a review of isotopic paleoecology of the genus *Coelodonta* from the Tibetan Plateau to northern Eurasia. Front. Ecol. Evol. 12, 1377000.
Ma, J., Jiangzuo, Q., Jin, Z., Deng, G., Chen, Y., Yan, Y., 2025. Isotopic paleoecology of Ursidae from Hualongdong. Acta Anthropol. Sin. 44, 884–894 (in Chinese with English abstract).
MacCullough, D.R., Takatsuki, S., Kaji, K. (Eds.), 2009. Sika Deer: Biology and Management of Native and Introduced Populations. Springer, Tokyo, Tokyo.
Maslin, M.A., Brierley, C.M., Milner, A.M., Shultz, S., Trauth, M.H., Wilson, K.E., 2014. East African climate pulses and early human evolution. Quat. Sci. Rev. 101, 1–17.
Ni, X., Ji, Q., Wu, W., Shao, Q., Ji, Y., Zhang, C., Liang, L., Ge, J., Guo, Z., Li, J., Li, Q., Grün, R., Stringer, C., 2021. Massive cranium from Harbin in northeastern China establishes a new Middle Pleistocene human lineage. Innovation 2, 100130.
Norton, C.J., Braun, D.R. (Eds.), 2011. Asian Paleoanthropology: from Africa to China and Beyond, Vertebrate Paleobiology and Paleoanthropology. Springer, Netherlands, Dordrecht.
O'Leary, M.H., 1981. Carbon isotope fractionation in plants. Phytochemistry 20, 553–567.
Passey, B.H., Robinson, T.F., Ayliffe, L.K., Cerling, T.E., Sponheimer, M., Dearing, M.D., Roeder, B.L., Ehleringer, J.R., 2005. Carbon isotope fractionation between diet, breath CO_2, and bioapatite in different mammals. J. Archaeol. Sci. 32, 1459–1470.
Passey, B.H., Cerling, T.E., Levin, N.E., 2007. Temperature dependence of oxygen isotope acid fractionation for modern and fossil tooth enamels. Rapid Commun. Mass Spectrom. 21, 2853–2859.
Pearson, O.M., 2013. Hominin evolution in the Middle-Late Pleistocene: fossils, adaptive scenarios, and alternatives. Curr. Anthropol. 54, S221–S233.
Pederzani, S., Britton, K., 2019. Oxygen isotopes in bioarchaeology: principles and applications, challenges and opportunities. Earth Sci. Rev. 188, 77–107.
Pei, S., Cai, Y., Dong, Z., Tong, H., Sheng, J., Jin, Z., Wu, X., Liu, W., 2022. Evolution of cave system at Hualongdong, Anhui and its relation to human occupation. Acta Anthropol. Sin. 41, 593 (in Chinese with English abstract).
Pei, S., Dong, Z., Geng, S., Ye, Z., Ma, D., Zhang, Y., Jin, Z., 2025. Lithic assemblage and adaptive behaviors of hominins at Hualongdong site. Acta Anthropol. Sin. 44, 765–778 (in Chinese with English abstract).
Pellegrini, M., Snoeck, C., 2016. Comparing bioapatite carbonate pre-treatments for isotopic measurements: part 2 — impact on carbon and oxygen isotope compositions. Chem. Geol. 420, 88–96.
Pushkina, D., Bocherens, H., Chaimanee, Y., Jaeger, J.J., 2010. Stable carbon isotope reconstructions of diet and paleoenvironment from the late Middle Pleistocene Snake Cave in Northeastern Thailand. Naturwissenschaften 97, 299–309.
Puspaningrum, M.R., van den Bergh, G.D., Chivas, A.R., Setiabudi, E., Kurniawan, I., 2020. Isotopic reconstruction of Proboscidean habitats and diets on Java since the early Pleistocene: implications for adaptation and extinction. Quat. Sci. Rev. 228, 106007.
QGIS Development Team, 2024. QGIS Geographic Information System. QGIS Association.
Qin, Z., Sun, X., 2023. Glacial–interglacial cycles and early human evolution in China. Land 12, 1683.
Quade, J., Cerling, T.E., Andrews, P., Alpagut, B., 1995. Paleodietary reconstruction of Miocene faunas from Paşalar, Turkey using stable carbon and oxygen isotopes of fossil tooth enamel. J. Hum. Evol. 28, 373–384.
R Core Team, 2025. R: a Language and Environment for Statistical Computing. R Foundation for Statistical Computing, Vienna, Austria.
Roberts, P., Petraglia, M., 2015. Pleistocene rainforests: barriers or attractive environments for early human foragers? World Archaeol. 47, 718–739.
Roberts, P., Stewart, M., Alagaili, A.N., Breeze, P., Candy, I., Drake, N., Groucutt, H.S., Scerri, E.M.L., Lee-Thorp, J., Louys, J., Zalmout, I.S., Al-Mufarreh, Y.S.A., Zech, J., Alsharekh, A.M., Omari, A. al, Boivin, N., Petraglia, M., 2018. Fossil herbivore stable isotopes reveal middle Pleistocene hominin palaeoenvironment in 'Green Arabia'. Nat. Ecol. Evol. 2, 1871–1878.
Shaikh, S., Bocherens, H., Suraprasit, K., 2025. Stable isotope ecology of Quaternary cervid and bovid species in Southeast Asia with implications for wildlife conservation. Sci. Rep. 15, 3939.
Sharp, Z.D., Cerling, T.E., 1998. Fossil isotope records of seasonal climate and ecology: straight from the horse's mouth. Geology 26, 219–222.
Smith, B.N., Epsten, S., 1971. Two categories of $^{13}C/^{12}C$ ratios for higher plants. Plant Physiol. 47, 380–384.
Snoeck, C., Pellegrini, M., 2015. Comparing bioapatite carbonate pre-treatments for isotopic measurements: part 1—Impact on structure and chemical composition. Chem. Geol. 417, 394–403.
Sponheimer, M., Lee-Thorp, J.A., 1999. Oxygen isotopes in enamel carbonate and their ecological significance. J. Archaeol. Sci. 26, 723–728.
Sponheimer, M., Lee-Thorp, J.A., 2001. The oxygen isotope composition of mammalian enamel carbonate from Morea Estate, South Africa. Oecologia 126, 153–157.
Stacklyn, S., Wang, Yang, Jin, C., Wang, Yuan, Sun, F., Zhang, C., Jiang, S., Deng, T., 2017. Carbon and oxygen isotopic evidence for diets, environments and niche differentiation of early Pleistocene pandas and associated mammals in South China. Palaeogeogr. Palaeoclimatol. Palaeoecol. 468, 351–361.
Stefaniak, K., Stachowicz-Rybka, R., Borówka, R.K., Hrynowiecka, A., Sobczyk, A., Moskal-del Hoyo, M., Kotowski, A., Nowakowski, D., Krajcarz, M.T., Billia, E.M.E., Persico, D., Burkanova, E.M., Leshchinskiy, S.V., van Asperen, E., Ratajczak, U., Shpansky, A.V., Lempart, M., Wach, B., Niska, M., van der Made, J., Stachowicz, K., Lenarczyk, J., Piątek, J., Kovalchuk, O., 2021. Browsers, grazers or mix-feeders? Study of the diet of extinct Pleistocene Eurasian forest rhinoceros *Stephanorhinus kirchbergensis* (Jäger, 1839) and woolly rhinoceros *Coelodonta antiquitatis* (Blumenbach, 1799). Quat. Int. 605–606, 192–212.
Sternberg, L. da S.L., 1989. Oxygen and hydrogen isotope ratios in plant cellulose: mechanisms and applications. In: Stable Isotopes in Ecological Research. Springer, New York, pp. 124–141.
Suga, S., 1979. Comparative histology of progressive mineralization pattern of developing incisor enamel of rodents. J. Dent. Res. 58, 1025–1026.
Sun, F., Wang, Yang, Wang, Yuan, Jin, C., Deng, T., Wolff, B., 2019. Paleoecology of Pleistocene mammals and paleoclimatic change in South China: evidence from stable carbon and oxygen isotopes. Palaeogeogr. Palaeoclimatol. Palaeoecol. 524, 1–12.
Suraprasit, K., Bocherens, H., Chaimanee, Y., Panha, S., Jaeger, J.J., 2018. Late Middle Pleistocene ecology and climate in Northeastern Thailand inferred from the stable isotope analysis of Khok Sung herbivore tooth enamel and the land mammal cenogram. Quat. Sci. Rev. 193, 24–42.
Suraprasit, K., Jaeger, J.J., Shoocongdej, R., Chaimanee, Y., Wattanapituksakul, A., Bocherens, H., 2020. Long-term isotope evidence on the diet and habitat breadth of Pleistocene to Holocene Caprines in Thailand: implications for the extirpation and conservation of Himalayan gorals. Front. Ecol. Evol. 8, 67.

Suraprasit, K., Shoocongdej, R., Wattanapituksakul, A., Chintakanon, K., Bocherens, H., 2024. The late occurrence of specialized hunter-gatherer occupation of tropical rainforests in Pang Mapha, northwestern Thailand. Quat. Sci. Rev. 329, 108573.
Tejada, J.V., Flynn, J.J., Antoine, P.O., Pacheco, V., Salas-Gismondi, R., Cerling, T.E., 2020. Comparative isotope ecology of western Amazonian rainforest mammals. Proc. Natl. Acad. Sci. 117, 26263–26272.
Tejada-Lara, J.V., MacFadden, B.J., Bermudez, L., Rojas, G., Salas-Gismondi, R., Flynn, J. J., 2018. Body mass predicts isotope enrichment in herbivorous mammals. Proc. R. Soc. B Biol. Sci. 285, 20181020.
Tong, H., Wu, X., Sheng, J., Jin, Z., Pei, S., Wu, L., 2018. Preliminary report on the mammalian fossils from the ancient human site of Hualong Cave in DongZhi, Anhui. Acta Anthropol. Sin. 23, 284–305 (in Chinese with English abstract).
Tong, H., Zhang, B., Wu, X., Qu, S., 2019. Mammalian fossils from the Middle Pleistocene human site of Bailongdong in Yunxi, Hubei. Acta Anthropol. Sin. 38, 613–640 (in Chinese with English abstract).
Tong, H., Jiangzuo, Q., Li, Q., Chang, M., Liu, B., Jin, Z., 2025. New mammalian fossils from the Hualongdong Site. Acta Anthropol. Sin. 779–798 (in Chinese with English abstract).
Tougard, C., Jaeger, J.J., Chaimanee, Y., Suteethorn, V., Triamwichanon, S., 1998. Discovery of a *Homo* sp. tooth associated with a mammalian cave fauna of late Middle Pleistocene age, Northern Thailand. J. Hum. Evol. 35, 47–54.
Troughton, J.H., Card, K.A., 1975. Temperature effects on the carbon-isotope ratio of C_3, C_4 and crassulacean-acid-metabolism (CAM) plants. Planta 123, 185–190.
Tsutaya, T., Sawafuji, R., Taurozzi, A.J., Fagernäs, Z., Patramanis, I., Troché, G., Mackie, M., Gakuhari, T., Oota, H., Tsai, C.H., Olsen, J.V., Kaifu, Y., Chang, C.H., Cappellini, E., Welker, F., 2025. A male Denisovan mandible from Pleistocene Taiwan. Science 388, 176–180.
van der Merwe, N.J., Medina, E., 1991. The canopy effect, carbon isotope ratios and foodwebs in Amazonia. J. Archaeol. Sci. 18, 249–259.
Wang, W., Potts, R., Baoyin, Y., Huang, W., Cheng, H., Edwards, R., Ditchfield, P., 2007. Sequence of mammalian fossils, including hominoid teeth, from the Bubing Basin caves, South China. J. Hum. Evol. 52, 370–379.
Wang, Yongjin, Cheng, H., Edwards, R.L., Kong, X., Shao, X., Chen, S., Wu, J., Jiang, X., Wang, X., An, Z., 2008. Millennial- and orbital-scale changes in the East Asian monsoon over the past 224,000 years. Nature 451, 1090–1093.
Wang, Yang, Wang, X.M., Xu, Y.F., Zhang, C.F., Li, Q., Tseng, Z.J., Takeuchi, G., Deng, T., 2008. Stable isotopes in fossil mammals, fish and shells from Kunlun Pass Basin, Tibetan Plateau: Paleo-climatic and paleo-elevation implications. Earth Planet Sci. Lett. 270, 73–85.
White, T.D., Asfaw, B., DeGusta, D., Gilbert, H., Richards, G.D., Suwa, G., Clark Howell, F., 2003. Pleistocene *Homo sapiens* from middle awash, Ethiopia. Nature 423, 742–747.
Wickham, H., 2011. ggplot2. Wiley interdiscip. Rev. Comput. Stat. 3, 180–185.
Wright, L.E., Schwarcz, H.P., 1998. Stable carbon and oxygen isotopes in human tooth enamel: identifying breastfeeding and weaning in prehistory. Am. J. Phys. Anthropol. 106, 1–18.
Wright, L.E., Schwarcz, H.P., 1999. Correspondence between stable carbon, oxygen and nitrogen isotopes in human tooth enamel and dentine: infant diets at Kaminaljuyu. J. Archaeol. Sci. 26, 1159–1170.
Wu, R., Li, X., Wu, X., Mu, X., 2002. *Homo erectus* from Nanjing. Jiangsu Science and Technology. Publishing House, Nanjing (in Chinese with English abstract).
Wu, X., Pei, S., Cai, Y., Tong, H., Li, Q., Dong, Z., Sheng, J., Jin, Z., Ma, D., Xing, S., Li, X., Cheng, X., Cheng, H., de la Torre, I., Edwards, R.L., Gong, X.C., An, Z.S., Trinkaus, E., Liu, W., 2019. Archaic human remains from Hualongdong, China, and Middle Pleistocene human continuity and variation. Proc. Natl. Acad. Sci. 116, 9820–9824.
Wu, X., Pei, S., Cai, Y., Tong, H., Xing, S., Jashashvili, T., Carlson, K.J., Liu, W., 2021. Morphological description and evolutionary significance of 300 ka hominin facial bones from Hualongdong, China. J. Hum. Evol. 161, 103052.
Wu, X., Martinón-Torres, M., Xing, S., Pei, S., Cai, Y., Tong, H., Bermúdez De Castro, J. M., Liu, W., 2025. The hominin teeth from the late Middle Pleistocene Hualongdong site, China. J. Hum. Evol. 206, 103727.
Xing, S., Wu, X., Liu, W., Pei, S., Cai, Y., Tong, H., Trinkaus, E., 2021. Middle Pleistocene human femoral diaphyses from Hualongdong, Anhui Province, China. Am. J. Phys. Anthropol. 174, 285–298.
Xu, C., Zhang, Y., Chen, C., Fang, D., 1984. Human occipital bone and mammalian fossils from Chaoxian, Anhui. Acta Anthropol. Sin. 3, 202–209 (in Chinese with English abstract).
Yakir, D., 1992. Variations in the natural abundance of oxygen-18 and deuterium in plant carbohydrates. Plant Cell Environ. 15, 1005–1020.
Yan, Y., Wang, Y., Zhu, M., Zhang, Y., Qin, D., Jin, C., 2023. New rhino remains from Middle to late Pleistocene of Chongzuo, Guangxi with discussion on Quaternary Rhinoceros evolution in Southern China. Quat. Sci. 43, 777–792 (in Chinese with English abstract).
Yang, S.L., Ding, Z.L., Wang, X., Tang, Z.H., Gu, Z.Y., 2012. Negative $\delta^{18}O$–$\delta^{13}C$ relationship of pedogenic carbonate from northern China indicates a strong response of C_3/C_4 biomass to the seasonality of Asian monsoon precipitation. Palaeogeogr. Palaeoclimatol. Palaeoecol. 317–318, 32–40.
Yang, S.X., Wang, F.G., Xie, F., Yue, J.P., Deng, C.L., Zhu, R.X., Petraglia, M.D., 2021. Technological innovations at the onset of the Mid-Pleistocene Climate Transition in high-latitude East Asia. Natl. Sci. Rev. 8 nwaa053.
Zeitoun, V., Winayalai, C., Auetrakulvit, P., Debruyne, R., Mallye, J.-B., Lenoble, A., 2023. Transgressing the limits of palaeoenvironmental data for Southeast Asian Pleistocene faunal assemblages: a critical review to go further. Ann. Paleontol. 109, 102657.
Zeller, E., Timmermann, A., Yun, K.S., Raia, P., Stein, K., Ruan, J., 2023. Human adaptation to diverse biomes over the past 3 million years. Science 380, 604–608.
Zhang, Yijing, Fan, Y., Yao, Y., Tian, C., Liang, H., Li, J., Liao, W., Bae, C.J., Wang, W., 2024. Variation in the Quaternary *Stegodon-Ailuropoda* faunal complex in Southern China: upper pubu Cave (Bubing Basin, Guangxi). Quat. Sci. Rev. 346, 109082.
Zhang, Yingqi, Westaway, K.E., Haberle, S., Lubeek, J.K., Bailey, M., Ciochon, R., Morley, M.W., Roberts, P., Zhao, J., Duval, M., Dosseto, A., Pan, Y., Rule, S., Liao, W., Gully, G.A., Lucas, M., Mo, J., Yang, L., Cai, Y., Wang, W., Joannes-Boyau, R., 2024. The demise of the giant ape *Gigantopithecus blacki*. Nature 625, 535–539.
Zheng, L., Huang, W., 2001. Hexian Hominid Site. Zhonghua Book Company, Beijing (in Chinese with English abstract).